

AERODYNAMICS OF VEHICLES IN FINITE LENGTH TUBES

Andrew G. Hammitt



APRIL 1974

FINAL REPORT

Reproduced by
NATIONAL TECHNICAL
INFORMATION SERVICE
U S Department of Commerce
Springfield VA 22151

Document is available to the public through the
National Technical Information Service,
Springfield, Virginia 22151

Prepared for

DEPARTMENT OF TRANSPORTATION
FEDERAL RAILROAD ADMINISTRATION
Office of Research, Development and Demonstrations
Washington, D.C. 20590

1. Report No. FRA-ORD&D-74-10		2. Government Accession No.		3. Recipient's Catalog No. PB 236 692	
4. Title and Subtitle THE AERODYNAMICS OF VEHICLES IN FINITE LENGTH TUBES				5. Report Date April 1974	
				6. Performing Organization Code	
7. Author(s) Andrew G. Hammitt				8. Performing Organization Report No. 96034-L014-0	
9. Performing Organization Name and Address TRW Transportation and Environmental Operations One Space Park Redondo Beach, California 90278				10. Work Unit No.	
				11. Contract or Grant No. DOT-FR-30004	
12. Sponsoring Agency Name and Address Office of Research, Development and Demonstrations Federal Railroad Administration U. S. Department of Transportation 2100 2nd Street, S.W., Washington, D.C. 20590				13. Type of Report and Period Covered Final September 1972 - October 1973	
				14. Sponsoring Agency Code	
15. Supplementary Notes Related reports include "Aerodynamic Analysis of Vehicles in Tubes," A. G. Hammitt, et al., April 1968 (PB 178 796), "An Analytical Procedure for Calculating the Aerodynamic Performance of Vehicles Traveling in Tunnels," C. R. Strom, December 1972 (PB 220 082) and other DOT sponsored studies referenced herein.					
16. Abstract High speed vehicles may operate in tunnels or tubes to minimize impact on the surrounding environment. Operation in tunnels or tubes minimizes the impact of surface obstacles, high noise levels, weather constraints and street congestion in metropolitan areas. The performance of these vehicles is significantly affected by the aerodynamics and need to be understood. The aerodynamics of vehicles traveling through tubes are significantly affected by the constraints of the tube wall and the relative size (blockage ratio) of the vehicle. Steady flow conditions are reached only after long travel times. In this report, the flow created by vehicle travel in a tube is analyzed using numerical integration of the unsteady flow equations. Steady state conditions are rarely obtained for closed-end tubes up to several hundred miles in length. Solutions are presented for various blockage ratio vehicles with choked and unchoked flow conditions about them. Various tube lengths are also considered. The solution for a doubly infinite tube is found to be approaching the asymptotic long time solution.					
17. Key Words Tunnels Tube Vehicle Systems Aerodynamics High Speed Ground Transportation			18. Distribution Statement Copies may be purchased from: NATIONAL TECHNICAL INFORMATION SERVICE (NTIS) U. S. Department of Commerce Springfield, Virginia 22151		
19. Security Classif. (of this report) Unclassified		20. Security Classif. (of this page) Unclassified		21. No. of Pages 86	22. Price



CONTENTS

ABSTRACT	i
NOMENCLATURE	vii
1. INTRODUCTION	1
2. NEAR FLOWFIELD	7
2.1 Effect of Heat Transfer and Fluid Velocity	9
2.2 Momentum Loss and Drag	11
2.3 Solutions for the Near Flowfield	12
3. FAR FLOWFIELD	21
3.1 Far Flowfield Results	22
4. CONCLUSIONS	59
APPENDIX A NEAR FLOWFIELD	61
APPENDIX B FAR FLOWFIELD SOLUTION	69
APPENDIX C EFFECT OF HEAT TRANSFER	79
REFERENCES	81

Preceding page blank

ILLUSTRATIONS

Figure

1	Schematic Diagram of Tube Vehicle Configuration . .	8
2	Supersonic Vehicle Base Flow Configuration.	10
3	Near Flow Field Drag and Momentum Loss Coefficients, $\beta = 0.5$	15
4	Near Flow Field Drag and Momentum Loss Coefficients, $\beta = 0.6$	16
5	Near Flow Field Drag and Momentum Loss Coefficients, $\beta = 0.7$	17
6	Near Flow Field Drag and Momentum Loss Coefficients, $\beta = 0.8$	18
7	Effect of Stagnation Temperature and Induced Velocity on Near Flow Field Drag and Momentum Loss Coefficients, $M_\infty = 0.2$ $\beta = 0.5$	19
8	Vehicle Travel as a Function of Time for the Various Cases Calculated.	24
9	Vehicle Velocity as a Function of Time for the Various Cases Calculated	25
10	Relative Mach Number as a Function of Time for Cases 1, 2, 4, 5, and 6	26
11	Drag, Drag Coefficient, and Momentum Loss Coefficient for Cases 1 and 2	27
12	Induced Velocity as a Function of Time for Cases 1 and 2	28
13	Entropy as a Function of Time for Cases 1 and 2 . .	29
14	Pressure as a Function of Time for Cases 1 and 2. .	30
15	Mass Flow Past the Vehicle Divided by Mass Swept- Out by Vehicle for Undisturbed Conditions as a Function of Time for Cases 1 and 4	31
16	Induced Velocity and Pressure as a Function of Distance Along the Tube at $t = 1000$ seconds, Case 1	32

ILLUSTRATIONS (CONTINUED)

Figure

17	Drag, Drag Coefficient, and Momentum Loss Coefficient as a Function of Time for Cases 4, 5, and 6	33
18	Induced Velocity as a Function of Time for Cases 4, 5, and 6	34
19	Entropy Velocity as a Function of Time for Cases 4, 5, and 6	35
20	Pressure Velocity as a Function of Time for Cases 4, 5, and 6	36
21	Entropy at the Closed Tube Ends In Front of and Behind the Vehicle as a Function of Time. . . .	37
22	Pressure of the Closed Tube Ends in Front of and Behind the Vehicle as a Function of Time. . . .	38
23	Relative Mach Number as a Function of Time for Cases 3 and 7	39
24	Drag, Drag Coefficient, and Momentum Loss Coefficient as a Function of Time for Cases 3 and 7	40
25	Induced Velocity as a Function of Time for Cases 3 and 7	41
26	Entropy as a Function of Time for Cases 3 and 7 . .	42
27	Pressure as a Function of Time for Cases 3 and 7. .	43
28	Induced Velocity as a Function of Position Along the Tube for Case 3	44
29	Entropy as a Function of Position Along the Tube for Case 3	45
30	Pressure as a Function of Position Along the Tube for Case 3	46
31	Induced Velocity as a Function of Position Along the Tube for Case 7	47

ILLUSTRATIONS (CONTINUED)

Figure

32	Entropy as a Function of Position Along the Tube for Case 7	48
33	Pressure as a Function of Position Along the Tube for Case 7	49
B-1	Friction Coefficient as a Function of Reynolds Number	72
B-2	Time-Distance Diagram of the Vehicle Boundary Condition for the Far Flow Field	74
B-3	Time-distance diagram illustrating the way in which different boundary conditions can be used to satisfy a variety of conditions from the same initial calculation.. . . .	77

TABLES

1	Conditions for Near Flow Field Solutions	13
2	Cases Computed for Far Flow Field Aerodynamics. . .	23

NOMENCLATURE

A	=	cross section area of tube
A_{vw}	=	vehicle surface area
A_{ww}	=	tube surface area
C_F	=	skin-friction coefficient
C_P	=	specific heat, at constant pressure
C	=	speed of sound
C_D	=	drag coefficient of vehicle based on tube area and relative velocity
C_H	=	Stanton number
d	=	tube diameter
D	=	drag of vehicle
F	=	friction force per unit volume
L	=	length of vehicle
m	=	mass flux
M_∞	=	vehicle Mach number
p	=	pressure
q_v	=	heat flux to vehicle
q_w	=	heat flux to wall
R	=	gas constant
Re_d	=	Reynolds number based on tube diameter and vehicle velocity
s	=	Entropy
t	=	time
T	=	Temperature
T_o	=	stagnation temperature of air
T_w	=	temperature of wall
T_{ow}	=	stagnation temperature at wall
T_{aw}	=	adiabatic wall temperature

NOMENCLATURE (CONTINUED)

- u = velocity of air relative to tube
- u_s = velocity of vehicle relative to tube
- v = velocity of air relative to vehicle, $v = u - u_s$
- x = distance along tube
- β = vehicle area blockage ratio, area of vehicle/area of tube
- γ = specific heat ratio
- λ = $\frac{2 C_f L}{(1 - d)}$
- ρ = fluid density
- τ_w = wall shear force
- τ_v = vehicle surface shear force

1. INTRODUCTION

Interest in high-speed tube vehicle systems gives increased importance to the aerodynamics of such vehicles. The restraint of the tube imposes a different condition than for vehicles in an open environment. The presence of the tube has two important effects: 1) it restricts the free passage of air about the vehicle, and 2) it confines the disturbances which originate at the vehicle from dissipating in three dimensions. Tube vehicle systems can be classified in many ways. For aerodynamic purposes, the most important parameters are the speed and blockage ratio of the vehicle, the tube length, and the means of propulsion. The importance of speed and blockage are obvious. If the tube is sufficiently long or the time of travel of the vehicle is sufficiently short, then the vehicle behavior will not be influenced by the tube ends. The type of propulsion system which is used has an important influence on the system design and the system aerodynamics. Vehicles drawn by a force from the tube wall are the type considered in this study and will be called externally propelled. It is convenient to consider the flowfield divided into two regions: 1) a far flowfield which covers the whole length of the tube excluding the region of the vehicle, and several tube diameters in front of and behind the vehicle; and 2) a near flowfield which covers this excluded region. The advantage of this division is that the far flowfield can be treated as a one-dimensional unsteady flow and the near flowfield as a steady flow field in vehicle-fixed coordinates and several space dimensions. For large L/d ratio vehicles, it will be found that a quasi-one-dimensional approach is adequate for the near flowfield.

The confinement of the tube walls has important effects upon the near flowfield. If the flow sufficiently far ahead of and behind the vehicle is considered, then the confining tube walls required that the mass flux (in vehicle-fixed coordinates) both ahead of and behind the vehicle are equal. The velocity or momentum flux relative to the vehicle must be the same, if the flow is incompressible; or increased behind the body, if the flow is compressible. A pressure drop across the vehicle is required to provide the drag force on the vehicle. This situation is identical to steady pipe flow where the drag of the walls causes the pressure to drop and, in the compressible case, the flow to accelerate.

The flow will be accelerated through the narrow annular passages about the vehicle with the result that it will reach Mach 1 for moderate flow Mach number ahead of the vehicle. The Mach number ahead of the vehicle, when choking in the annular passage occurs, is the maximum Mach number possible in front of the vehicle. When the flow about the vehicle is choked, then the flow conditions behind the vehicle can no longer influence those in front of the vehicle. The vehicle drag is no longer directly related to the vehicle characteristics, but more closely associated with the tube characteristics. In expanding from the sonic section, the flow may either accelerate to supersonic velocities and be shocked back to subsonic or diffuse smoothly to subsonic velocity. The process that actually occurs depends upon the downstream conditions just as in a convergent-divergent nozzle.

The near flowfield is coupled to the far flowfield. For the unchoked case, a pressure drop related to the vehicle drag provides the matching condition. For the choked case, matching of the relative Mach number is required. The far flowfield, when coupled to the near flowfield, determines the relative Mach number ahead of the vehicle for the unchoked case. For the choked case, the far flowfield determines the pressure ahead of and behind the vehicle, and the drag.

The far flowfield is caused by the vehicle starting transient. This transient causes pressure waves that propagate for long distances down the tube. The tube confines these waves so they cannot dissipate in three dimensions but are attenuated by heat transfer and friction with the tube walls. The far flowfield is essentially unsteady, but two simplified steady solutions (in correctly selected coordinate systems) can be obtained in both the limit of short and long time after the initiation of the vehicle motion. Soon after the vehicle has started, heat transfer and friction have not had time to affect the far flowfield, and the waves have only traveled a relatively short distance down the tube. The relatively weak waves caused by a vehicle moving with subsonic velocity are essentially isentropic. The flow across such waves can be described by one-dimensional steady relations, if a coordinate system moving with the waves is adopted. In the limit of very long times, the waves are completely dissipated by

friction and heat transfer, and the far flowfield becomes steady in a vehicle-fixed coordinate system. The pressure gradients in the tube are balanced by the friction on the tube walls. While these two steady solutions are available for short and long times (References 4 and 5) the intermediate time solutions are not steady in any coordinate system, and a solution to a one-dimensional unsteady flow problem with friction and heat transfer is required. These relations must be solved by numerical methods. The purpose of this study is to provide such numerical solutions.

The far flowfield is the mechanism which alleviates the need for all the fluid to flow through the annulus about the body. The body may push fluid ahead of it down the tube. If the body has low drag and blockage, then little fluid is pushed down the tube, and the fluid flows about the vehicle. If the flow is choked about the vehicle, a very severe limitation is imposed upon the rate of flow past the vehicle and fluid must be pushed ahead of it. There is no limit on maximum vehicle speed caused by the choking phenomena. The fluid is pushed ahead of the vehicle, as required, to cause any required Mach number relative to the vehicle.

The time required for the far flowfield to reach steady flow in a vehicle coordinate system depends upon the blockage. Consider an externally propelled vehicle which starts impulsively. A wave will be transmitted down the tube ahead of the vehicle. The wave reduces the Mach number relative to the vehicle to any value between the vehicle Mach number (no reduction) for a vehicle of zero drag and blockage, to zero relative Mach number for a vehicle which completely blocks the tube. As the vehicle progresses, the distance between the wave and vehicle increases, resulting in a larger amount of air moving with respect to the tube. Friction forces on this slug of moving air cause the pressure to increase from the wave front to the vehicle, and heat is transferred to the tube wall. For the case of a choked vehicle, the Mach number relative to the vehicle is constant, and the friction and heat transfer weaken the wave; but the pressure in front of the vehicle increases. This increased pressure causes an increased mass flow about the vehicle. This process continues until the mass flow about the vehicle reaches the amount of undisturbed flow swept out by the vehicle. When this condition is reached, the wave has attenuated to zero strength, and the amount of mass in the region affected by the far

flowfield is constant. The time or distance of vehicle travel before the flowfield becomes essentially constant depends upon the ratio between vehicle Mach number and relative fluid Mach number. If this ratio is near one, the time is near zero; but, if the ratio approaches ∞ , corresponding to a vehicle completely blocking the tube, the time approaches ∞ . For this reason, the asymptotic long-time solution is not useful for fully blocking vehicles. This process would be somewhat different, but essential features are similar for a vehicle that did not choke the flow.

The actual tube vehicle problem involves a vehicle in a tube traveling between two stations near the end of the tube with intermediate stops. The presence of and location of the ends of the tube, the acceleration and deceleration rate of the vehicle, and the location and duration of the intermediate stops all have an influence on the aerodynamics of the flow and the drag of the vehicle. If the vehicle starts at a station that is near the closed end of the tube, the pressure behind the vehicle will fall to a lower value than if the vehicle were not started near the closed end. All the fluid to fill the space behind the vehicle will have to pass around the vehicle because of the closed tube end behind. As the vehicle approaches the closed end of a tube, all the fluid must escape around the vehicle. An open end will allow the fluid to escape from the tube resulting in a different condition. As the vehicle runs down the tube a flowfield within the tube is generated. When the vehicle stops in a station, this flowfield is not immediately dissipated. When the vehicle accelerates from the station, flow conditions within the tube may not yet be ambient with the result that the forces on the vehicle may be different from those present if the conditions in the tube were ambient.

It is the purpose of this study to assess the magnitude and the importance of these effects. This assessment will be accomplished by considering two different vehicle configurations, one which results in choked flow at the speeds considered and one which does not. Three tube-end configurations are also considered, ends infinitely far from the vehicle in both directions, a closed end not far behind the vehicle's starting point, and a closed end not far ahead of the vehicle's stopping point. These cases should give an initial assessment of the effect of closed tube ends on the conditions in the tube.

The tube vehicle flowfield prediction program has now reached the state of development that it can be used to simulate actual tube vehicle systems performance. For instance, a vehicle traveling from New York to Washington with intermediate stops at Philadelphia and Baltimore could be considered. In this way the importance of aerodynamic effects in a real system could be evaluated. Once the relative importance of these basic effects are understood, a full exploration of all possible parameters is probably not justified because of the many possible variations. A better use of the capability would be to evaluate configurations of use to perform a particular mission.

This same capability can be used in other applications than the tube vehicle systems alone. The problem of a vehicle which normally operates in the open passing through tunnels at high speed or entering a tunnel under cities, stopping at a station, and then exiting from the other end of the tunnel are other applications of importance. A tunnel in which the vehicle proceeds at high speed through the entire tunnel will give somewhat different results from a tunnel in which the vehicle decelerates and stops in the middle of the tunnel. The most important aerodynamic effects are probably the vehicle drag and the pressure pulses caused by the vehicle. Tunnel contouring and flairing can be used to minimize the adverse features of these effects and minimize tunneling costs. Studies to date (References 1 and 2), have shown that these problems are best studied by a combination of approximate incompressible flow solutions and more exact compressible solutions. The drag effects are reasonably well predicted by the incompressible solution while compressible finite wave speed solutions are needed to give a good picture of the pressure pulses.



2. NEAR FLOWFIELD

The near flowfield describes the flow about the vehicle and extends over that distance in front of and behind the body in which the two dimensional nature or the change in cross sectional area of the flow must be taken into account. In most cases it can be considered to be steady flow with time varying boundary conditions. The flowfield is best considered in vehicle fixed coordinates as shown in Figure 1. The flow, relative to the vehicle, accelerates into the annular space between the vehicle and the tube. This flow is essentially isentropic and involves an increase in velocity and Mach number. The area ratio and relative Mach number ahead of the vehicle are limited to values that give a Mach number in the annular passage less than one. As the fluid flows throughout the annular passage, friction with the vehicle and the tube wall and heat transfer with the tube wall are all important effects. There can be no heat transfer with the vehicle unless the vehicle contains an energy source or sink. An energy source is quite possible for some configurations but will not be considered in this analysis. The combined effect of this heat transfer and friction is to increase the Mach number. A Mach number equal to one is the maximum value that can be reached at the exit from the annular passage. The flow then passes over the rear of the vehicle and eventually fills the entire tube behind the vehicle. In the ideal situation this flow over the back of the vehicle could be isentropic. This condition can be approached if a vehicle with a long pointed tail is used. If a blunt based vehicle is used, the flow will separate at the base. Under this condition the usual assumption, at least for low speed conditions, is that the base pressure is equal to the static pressure in the annulus at the base. Lower base pressures might be expected at higher vehicle Mach numbers.

If the flow through the annulus at the rear of the vehicle is at Mach number one, then the flow may expand supersonically into the base area and return to subsonic speeds through a variety of shock and mixing layer configurations. Under these conditions it is the downstream pressure and not the vehicle geometry that fixes the flow configuration. The base pressure

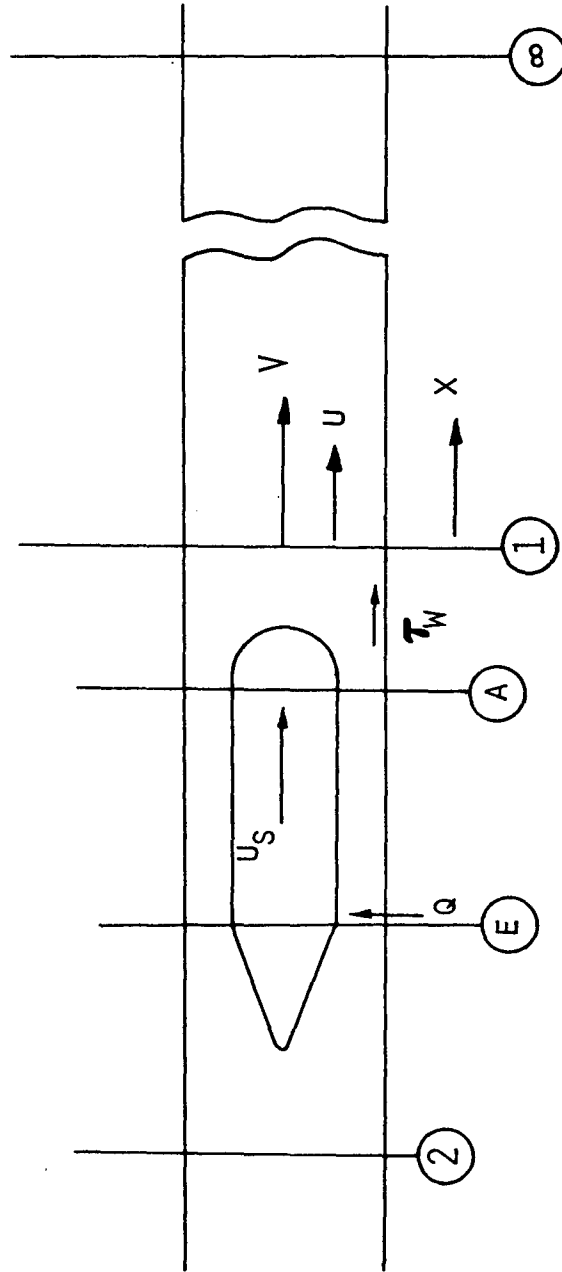


Figure 1. Schematic Diagram of Tube Vehicle Configuration

may be considerably reduced from the value at the annulus exit resulting in a higher vehicle drag. When the flow through the annulus has reached Mach number one at the exit, the choking condition, the relative Mach number in front of the vehicle is also fixed but the drag can have any value above a fixed minimum. When the flow in the annulus is subsonic, the vehicle drag is chiefly a function of the vehicle shape and the relative Mach number in front of the vehicle can vary to fit the required conditions. When the flow is sonic at the exit of the annulus, the relative Mach number is fixed by the vehicle geometry but the vehicle drag can adjust to accommodate the required conditions. The purpose of the near flowfield calculation then is to predict the drag as a function of relative Mach number for the unchoked conditions and the relative Mach number in front of the vehicle which causes choking.

The flow configuration behind the vehicle that occurs when the flow in the annulus is choked is a subject of some interest that will now be considered further. The important point to realize is that the pressure behind the vehicle after the flow has once again filled the tube and become uniform is set by downstream far flowfield and the local shock configuration has the flexibility to adjust to give these conditions. The actual flow configuration will depend very much on the trailing edge shape of the body but it is not necessary to determine it. In Reference 3, the assumption has been made that a normal shock exist along this tail of the body which would seem to require a body with a long pointed tail, (Figure 2). Although knowledge of shock wave boundary interactions shows that this is not a possible flow configuration except for a shock at low Mach number, it is of some use as a means of visualizing how a shock wave can adjust to match a required downstream condition. The assumption probably does not affect the accuracy of the solution for most conditions since the range of conditions that can be accommodated by allowing the normal shock wave to adjust over the available area ratios is quite large. However, there is no need to define the flow configuration in the base region and to do so complicates the problem.

2.1 EFFECT OF HEAT TRANSFER AND FLUID VELOCITY

While the drag coefficient of the vehicle is chiefly a function of the

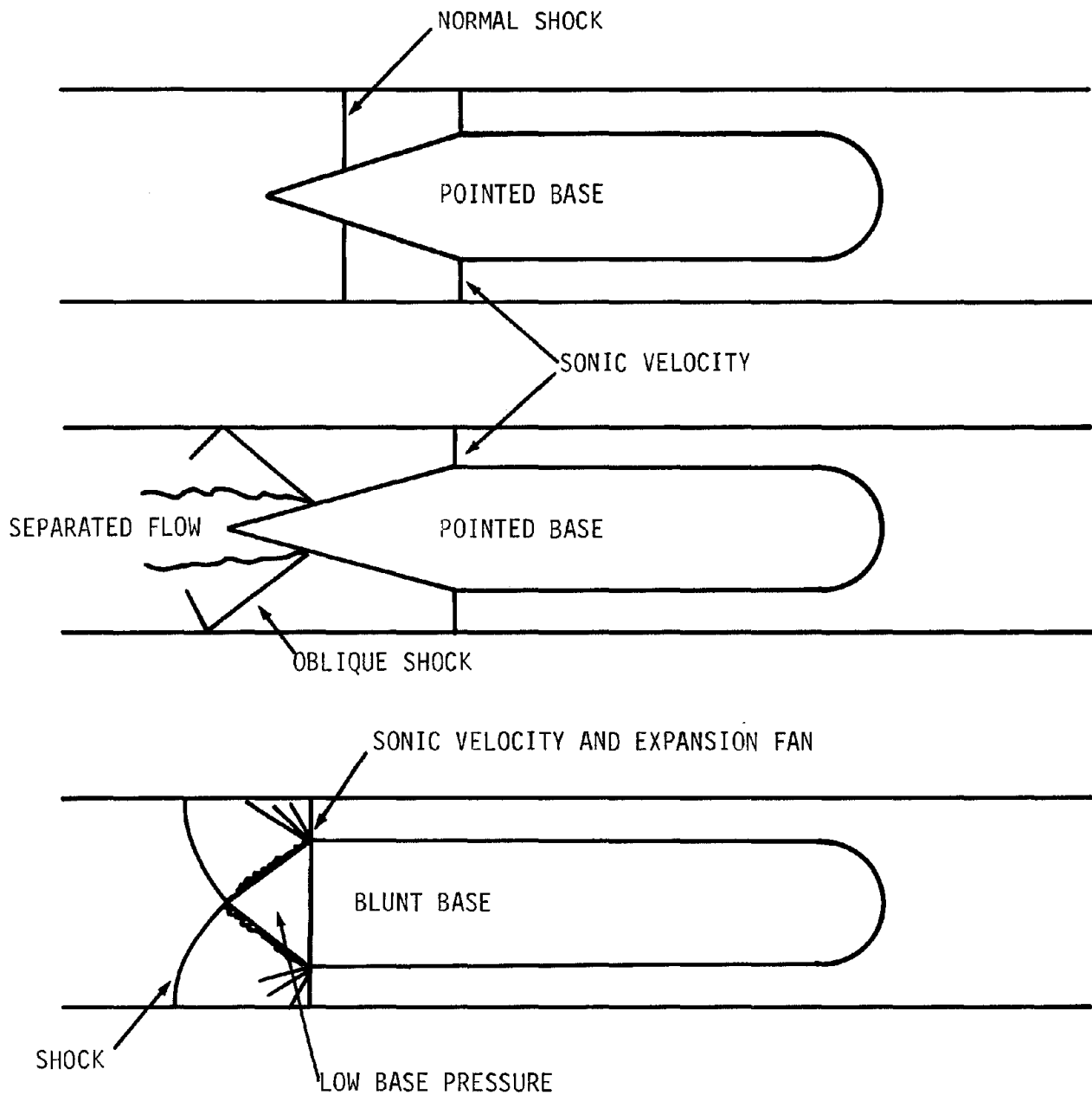


Figure 2. Supersonic Vehicle Base Flow Configurations

relative Mach number, the temperature of the fluid in front of the vehicle and the velocity of the fluid relative to the tube wall would both be expected to have some effect on the vehicle drag. It is shown in Appendix A that, if the flow is steady in vehicle fixed coordinates, the stagnation temperature of the fluid at which there is zero energy exchange with the tube wall is the stagnation temperature of fluid at wall temperature and velocity. If the vehicle is adiabatic, there is no energy transfer with the vehicle in the coordinate system fixed with the vehicle and the fluid flowing through the annular passage about the vehicle will approach the temperature in equilibrium with the wall. The temperature of the fluid ahead of the body will be higher than this equilibrium temperature if it has been heated by isentropic compression waves or shock waves so cooling will take place through the annular passage about the vehicle. The effect of the cooling is to reduce the velocity and Mach number and thereby the friction and drag.

If the fluid has a velocity with respect to the tube wall ahead of the vehicle, there is also an effect on the friction in the annular passage. In vehicle fixed coordinates, if the relative Mach number of the fluid with respect to the vehicle is constant, the effect of a velocity of the fluid with respect to the wall is to change the velocity of the tube wall with respect to the vehicle. If the fluid ahead of the vehicle has a component of velocity with respect to the tube in the direction of vehicle motion, as may be expected in most cases, then, in vehicle fixed coordinates, the velocity of the tube with respect to the vehicle is increased. The velocity difference between the tube wall and the fluid in the annular passage is decreased so that the friction on the tube wall is decreased resulting in a decrease in vehicle drag and increase in the relative Mach number which will cause choking.

2.2 MOMENTUM LOSS AND DRAG

The momentum loss by the fluid in flowing about the vehicle and the drag of the vehicle are not precisely the same quantity. The difference is the shear force on the tube wall along the annular passage about the vehicle. In general the momentum loss by the fluid will be somewhat larger than the drag of the body, but is possible to have the other situation when the average velocity of the fluid in the annular passage is in the same direction, with respect to the tube wall, as the direction of vehicle

travel. The friction on the tube wall has an influence on the drag of the vehicle by affecting the pressure drop through the annular passage, but the direct force on the tube wall contributes to the momentum loss of the fluid but not to the drag of the vehicle. The momentum loss to the fluid is the important quantity for determining the flowfield caused by the vehicle. Once the flowfield has been established, the drag of the vehicle can be determined directly from these flowfield parameters.

2.3 SOLUTIONS FOR THE NEAR FLOWFIELD

Calculations for the momentum loss and drag coefficients for vehicles of several blockage ratios and lengths are shown in Figures 3 through 6. These cases are all for conditions of zero fluid velocity and equilibrium temperature. For all these cases, the momentum loss coefficient is slightly larger than the drag coefficient. The character of the two curves is similar. As the Mach number increases from zero, they are relatively flat until the Mach number reaches an appreciable part of the choking Mach number. At that point, the momentum loss or drag coefficient starts to rise relatively rapidly and becomes vertical when it reaches the choking Mach number. At the choking Mach number, the coefficients can have any value above the minimum specified by these curves. However, the drag coefficient must always be less than the momentum loss coefficient by the same amount as at the choking Mach number.

These curves show the sensitivity of these coefficients and the choking Mach number to the value of the blockage ratio and friction. For high blockage ratio vehicles, the flow chokes at a relatively low relative Mach number, and the drag and momentum loss coefficients of the vehicle are quite high. Since some of the fluid is pushed down the tube ahead of the vehicle, the relative Mach number is not as high as the vehicle Mach number and the vehicle can proceed at speeds higher than the choking Mach number. Because of the reduced relative Mach number, the vehicle drag is not as high as the high drag coefficients might at first indicate. The various cases present in these figures are shown summarized in Table 1. The actual parameter that enters the calculation is the quantity

$$\lambda = \frac{2 C_f L}{(1 - d)}$$

Table 1				
Conditions for Near Flowfield Solutions				
Figure	β	λ	$\frac{L}{d}$	C_f
3	0.5	1	50	0.005
		0.1	10	0.0025
4	0.6	1	40	0.005
		0.1	8	0.0025
5	0.7	1	30	0.005
		0.1	6	0.0025
6	0.8	1	20	0.005
		0.25	5	0.005
		0.1	4	0.0025

and the drag for any combination of friction coefficient and vehicle length that gives this value of λ is described by the curves presented in Figures 3 through 6. Table 1 also contains typical values of friction coefficient and vehicle length for which these values of λ would be appropriate.

Figure 7 shows the effect of changes in temperature and induced fluid velocity on the momentum and drag loss coefficient. The range of the variables are probably twice as large as expected with a vehicle of this blockage ratio. For short vehicles, the effect is small, but it increases with increased vehicle length. The variation in the momentum loss coefficient and drag coefficient with changes in induced flow velocity and temperature was not considered for the vehicle used in this study since these effects are small and do not change the character of the results. However, these effects can easily be included and should be considered for longer vehicles where the effect would be of greater importance. The effect of temperature change and induced fluid velocity of the change in choking Mach number has not been investigated but might be expected to be of the same order.

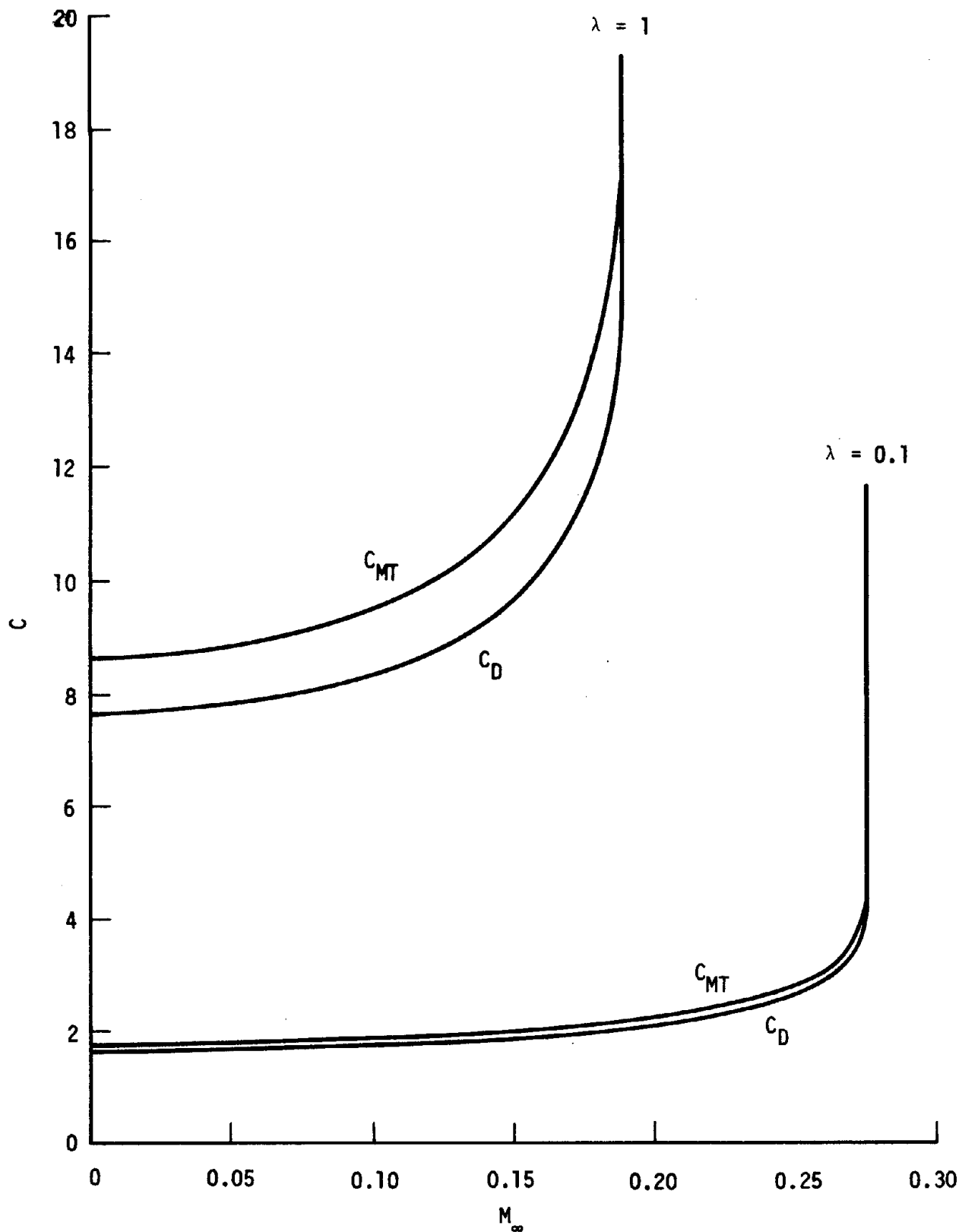


Figure 3. Near Flow Field Drag and Momentum Loss Coefficients, $\beta = 0.5$

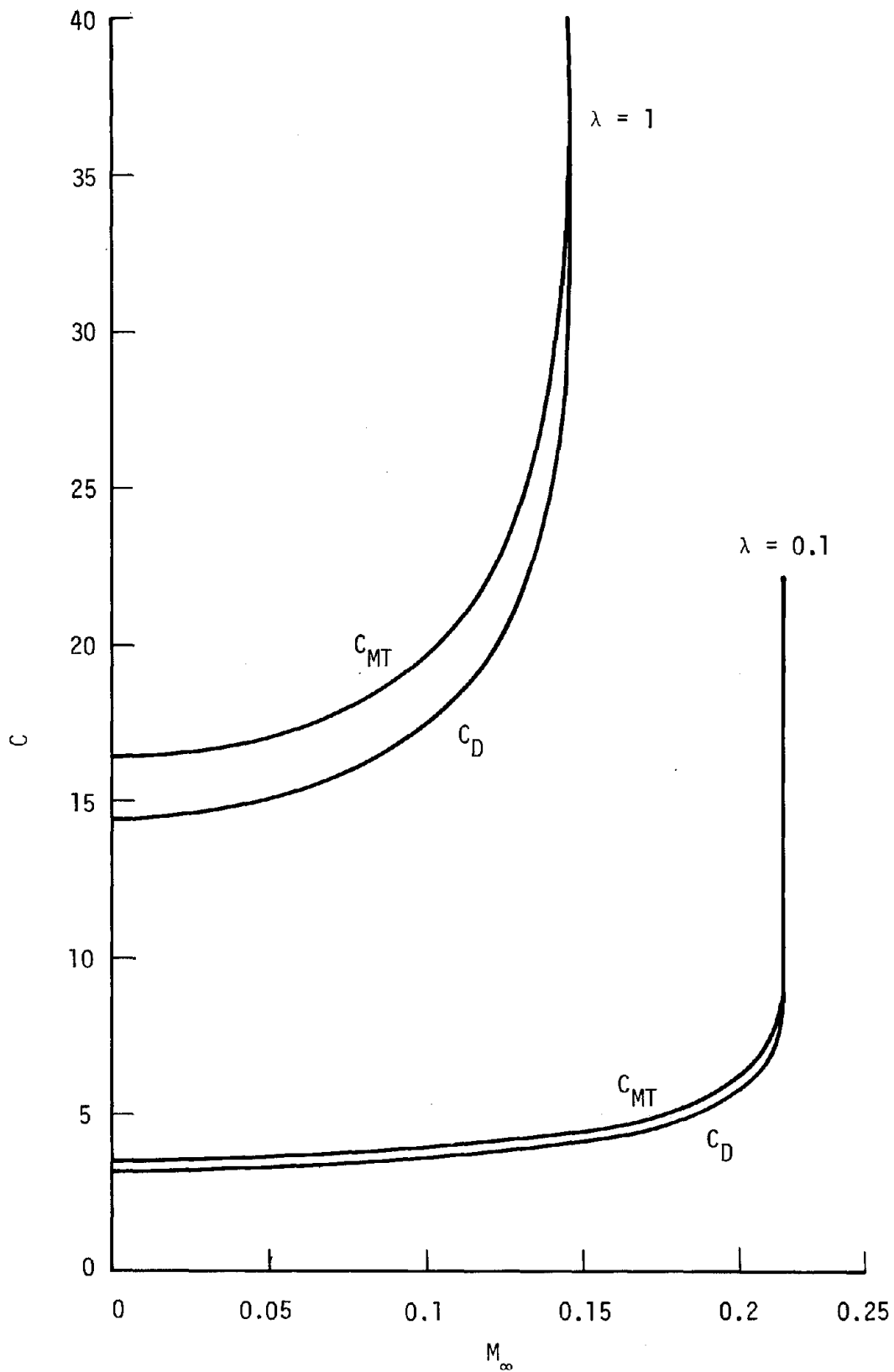


Figure 4. Near Flow Field Drag and Momentum Loss Coefficients, $\beta = 0.6$

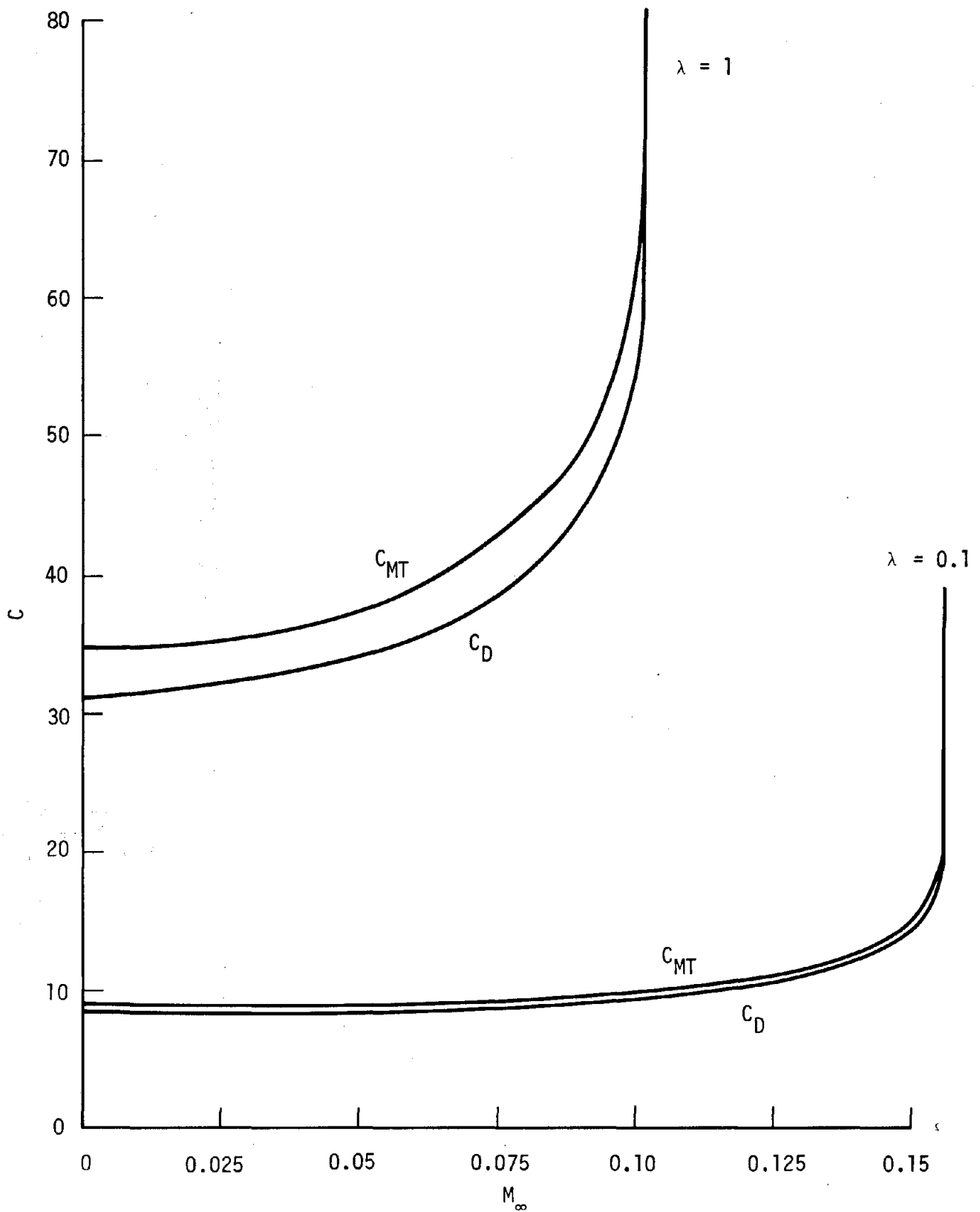


Figure 5. Near Flow Field Drag and Momentum Loss Coefficients, $\beta = 0.7$

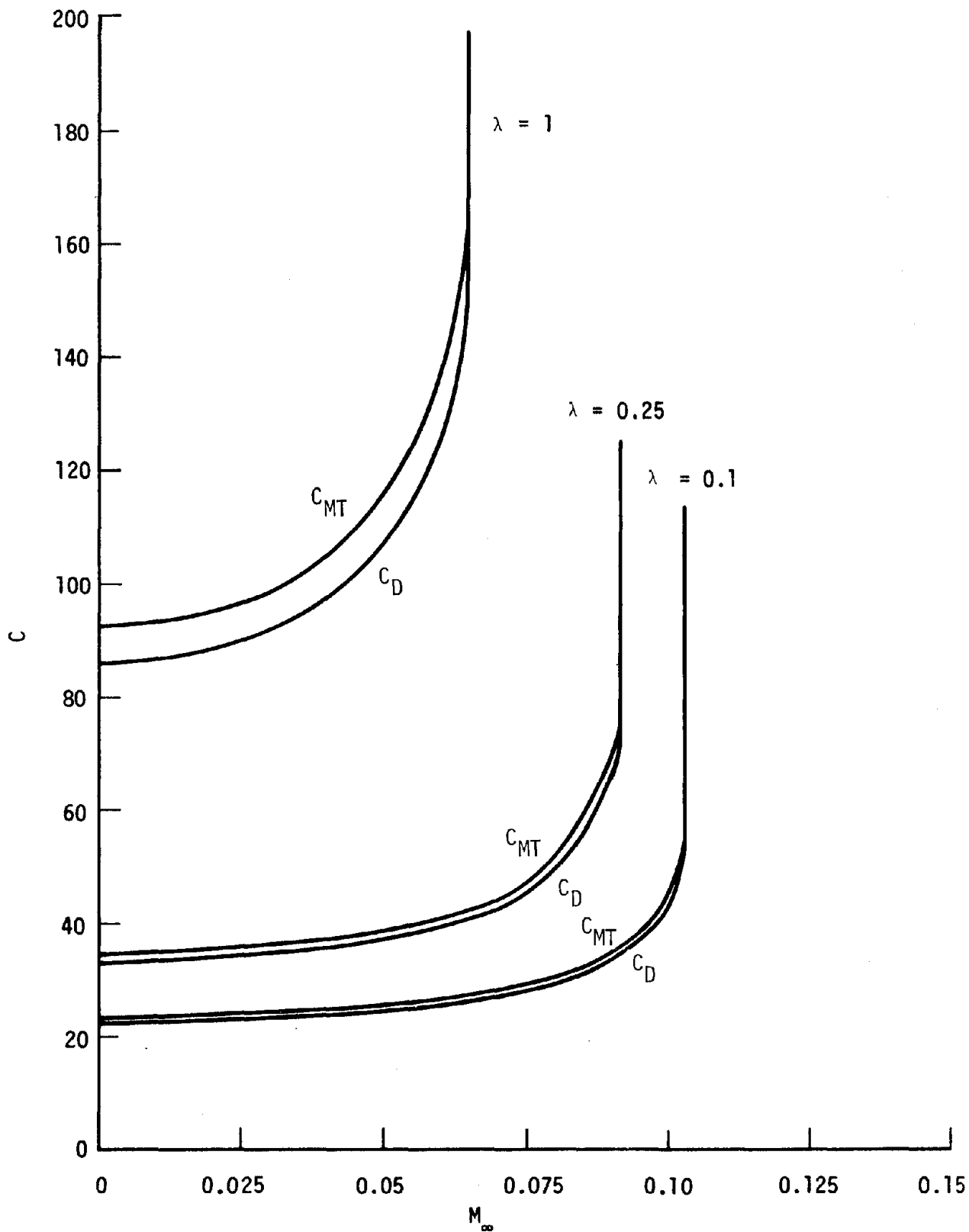


Figure 6. Near Flow Field Drag and Momentum Loss Coefficients, $\beta = 0.8$

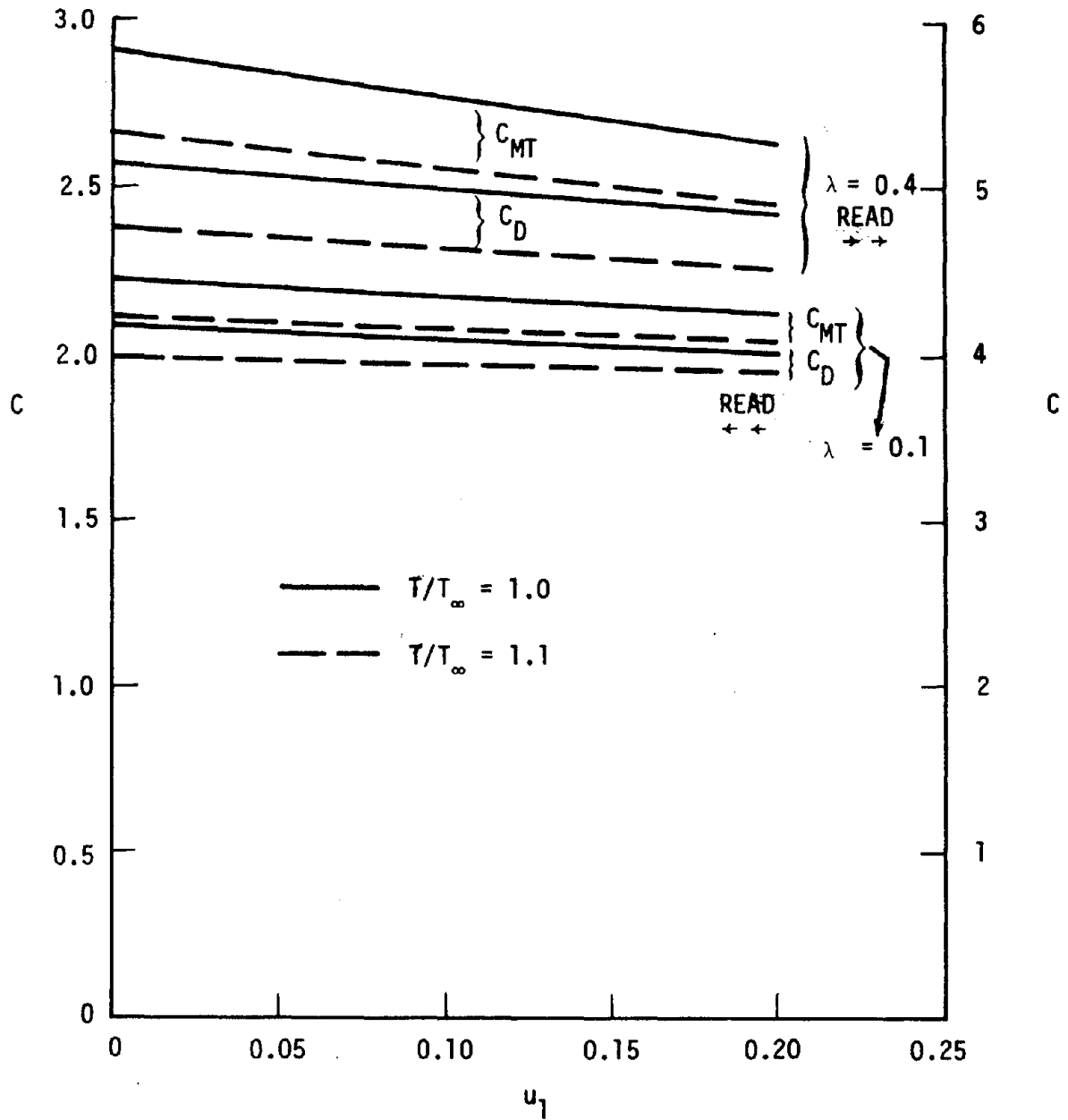


Figure 7. Effect of Stagnation Temperature and Induced Velocity on Near Flow Field Drag and Momentum Loss Coefficients. $M_\infty = 0.2$ $\beta = 0.5$



3. FAR FLOWFIELD

The far flowfield is that part of the flowfield which lies sufficiently far from the vehicle that it may be considered one dimensional. In the far flowfield the unsteady effects must be taken into account, but by considering regions away from the immediate vicinity of the body, two dimensional or area change effects may be neglected. The solution required is for one space dimensional unsteady flow including friction and heat transfer. This solution involves the integration of a partial differential equation in x and t and must be accomplished by numerical means. This integration can be performed by different means but the method used here is the integration along characteristic directions. An examination of the characteristic of the partial differential equations shows that there are certain special characteristic directions, those moving with the speed of sound with respect to the fluid and at fluid velocity, and that the integration of the partial differential equations can be reduced to the integration of total differential equations along these characteristic directions. A difficulty with this method is that the characteristic directions depend on the fluid properties so that the solution involves an iterative procedure in which a first estimate of the characteristic directions are determined, the solution for the fluid properties obtained, the characteristic direction redetermined, and the process continued until it converges.

Friction and heat transfer effects can be readily incorporated in this method without changing the form of the solution if it is assumed that the friction and heat transfer are determined only by the local values of the fluid properties themselves. This assumption is equivalent to assuming that the friction and heat transfer are the same as they would be in a steady flow with the same fluid properties and that the unsteady effects have no influences on these properties. For slow enough changes, these assumptions will be correct. A study of these unsteady effects was made in Reference 8 in connection with the tube vehicle problem. Using these results the conclusion is that the changes over most of the region of interest for the tube vehicle aerodynamics are slow enough so that the steady state assumption for determining the friction and heat transfer are adequate.

Over most of the range of interest the flow in the far flowfield will be turbulent. However, at the very low induced velocities which may exist

very far from the vehicle the flow will be laminar. The relation for the turbulent heat transfer coefficients give a finite Stanton number at zero velocity which would give zero heat transfer. This is because the heat conduction of the fluid is ignored and only the heat transferred by turbulent eddies is considered. Since the correct solution to the flow behind the train after a long enough time is that the temperature of the fluid be equal to the temperature of the tube wall, it is necessary to include the effects of laminar heat conduction to insure that this condition is actually achieved.

The thermal properties of the tube wall will have an effect on the heat transfer process within the tube. A complete solution to this problem would have to include an analysis of the heat transfer in the tube wall. However, if the tube wall is a very good conductor and heat sink, then its temperature will remain constant and if it is a very poor conductor and heat sink, the amount of heat transferred to the tube wall can be neglected. In Reference 5 an order of magnitude analysis of the tube wall heat transfer conditions was performed and the conclusion was reached that the tube wall would remain at an essentially constant temperature. Therefore, it is not necessary to analyze the tube wall heat transfer in detail and the fluid solution can be performed using the condition of constant tube wall temperature. A more detailed description of the method and equations used for the far flowfield solution is contained in Appendix B.

3.1 FAR FLOWFIELD RESULTS

The results of the various far flowfield calculations which have been performed are summarized in Table 2 and presented in Figures 8 through 33. The far flowfield is sufficiently complex and depends on such a variety of parameters that it is hard to present the results in a simple manner using a reasonable number of figures. These results can be used for two different purposes; first, to provide enough data so that a reasonable assessment can be made of the aerodynamic characteristics of different configurations and secondly to provide a better understanding of these characteristics to aid in the design of tube vehicle aerodynamic experiments. The cases selected for computation have been chosen to fit these two criterion and in addition Cases 3 and 7 which were specifically selected in conjunction with MITRE Corporation to provide comparisons between calculations to be performed by MITRE and the present calculations.

Table 2

Cases Computed for far Flowfield Aerodynamics

Case No.	Blockage Ratio	Vehicle Length (ft)	Vehicle Friction Coefficient	Closed Left End (ft)	Closed Right End (ft)	Vehicle Travel (ft)	End of Run Duration (sec)	Final Velocity (ft/sec)
1	0.5	100	.0025	-∞	+∞	280,000	1000	293
2	0.5	100	.0025	-2,000	+∞	58,500	214	293
3	0.5	50	.005	-5,000	45,000	40,000	173	0
4	0.8	40	.0025	-∞	+∞	229,000	800	293
5	0.8	40	.0025	-2,000	+∞	229,000	800	293
6	0.8	40	.0025	-2,000	232,000	230,000	822	0
7	0.8	50	.005	-5,000	45,000	40,000	173	0

Velocity for all runs - 8 ft/sec. acceleration to 293 ft/sec and constant velocity to end of run or deceleration at 8 ft/sec. at end of run.

Tube diameter - 10 ft., Initial tube pressure - 1 atmosphere

Vehicle starting position is $x = 0$, vehicle travels from left to right

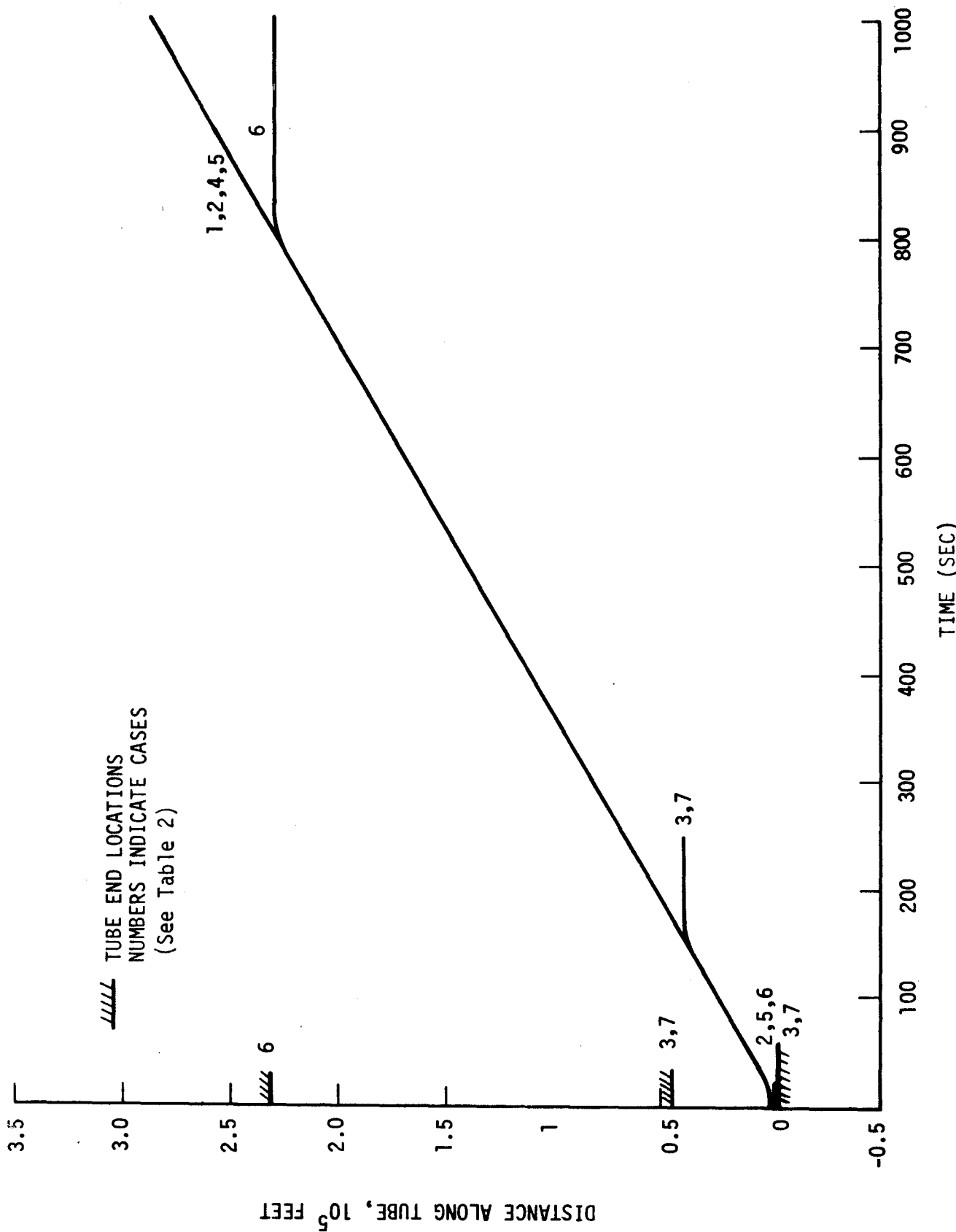


Figure 8. Vehicle Travel as a Function of Time for the Various Cases Calculated

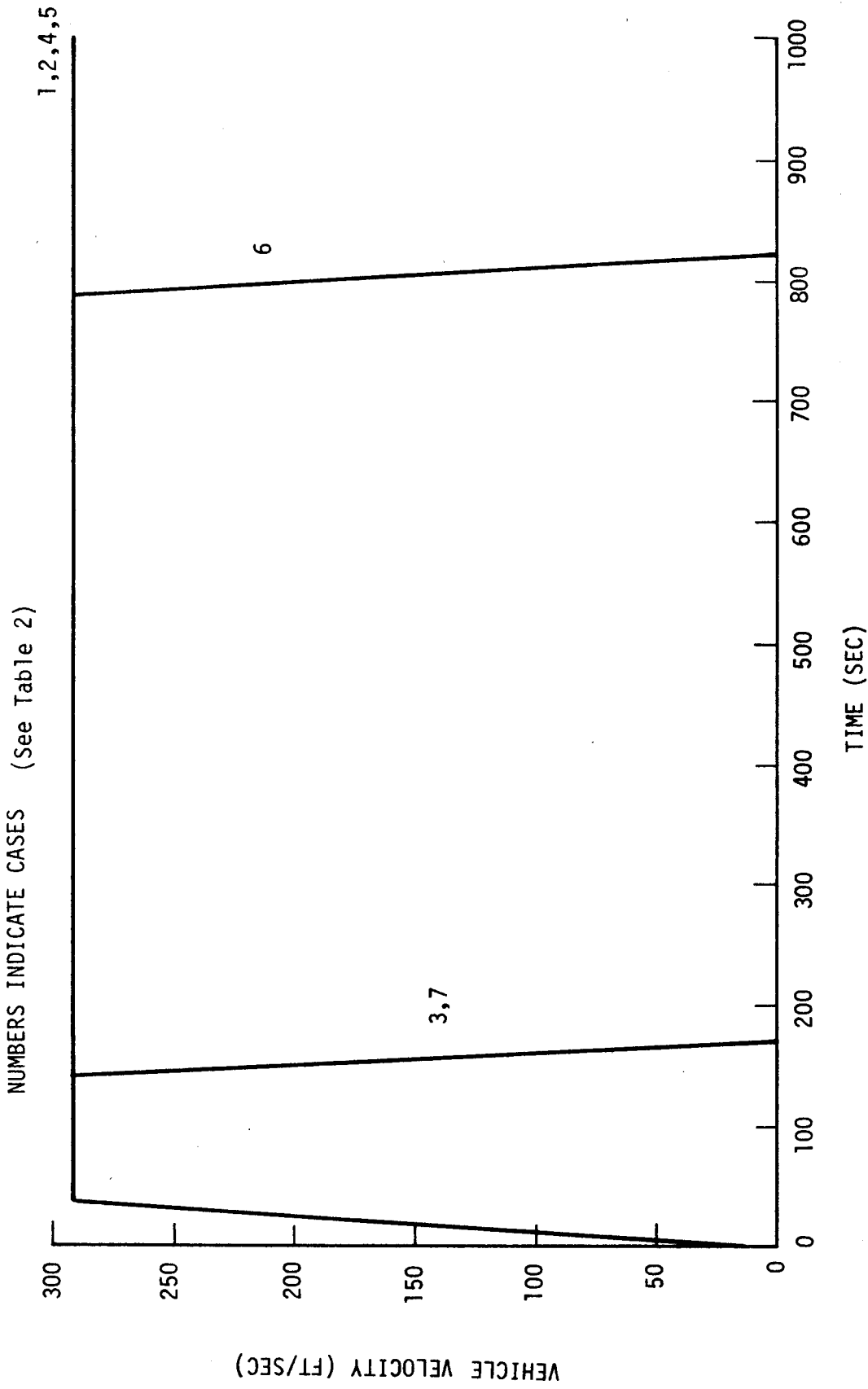


Figure 9. Vehicle Velocity as a Function of time for the Various Cases Calculated

NUMBERS INDICATE CASES (See Table 2)

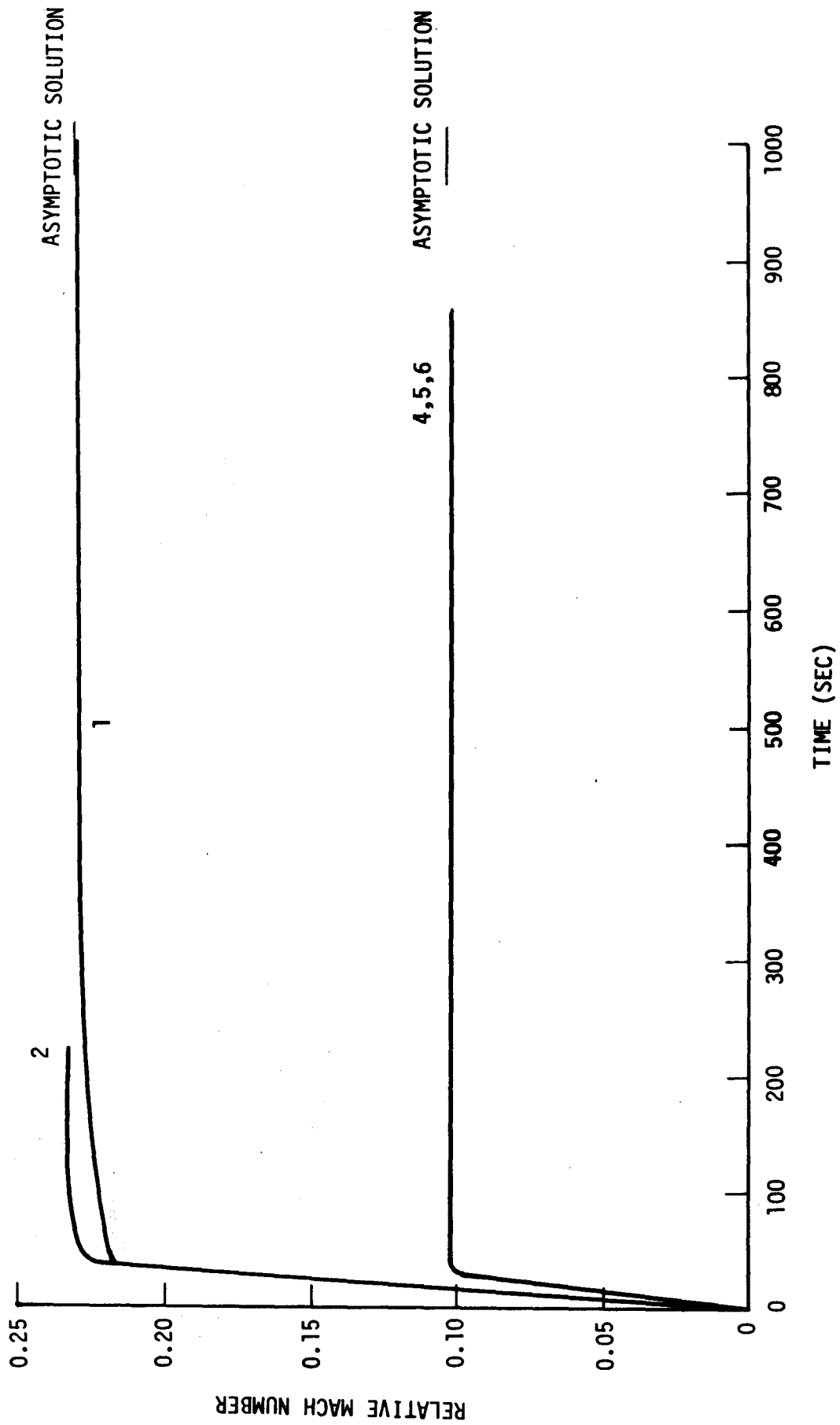
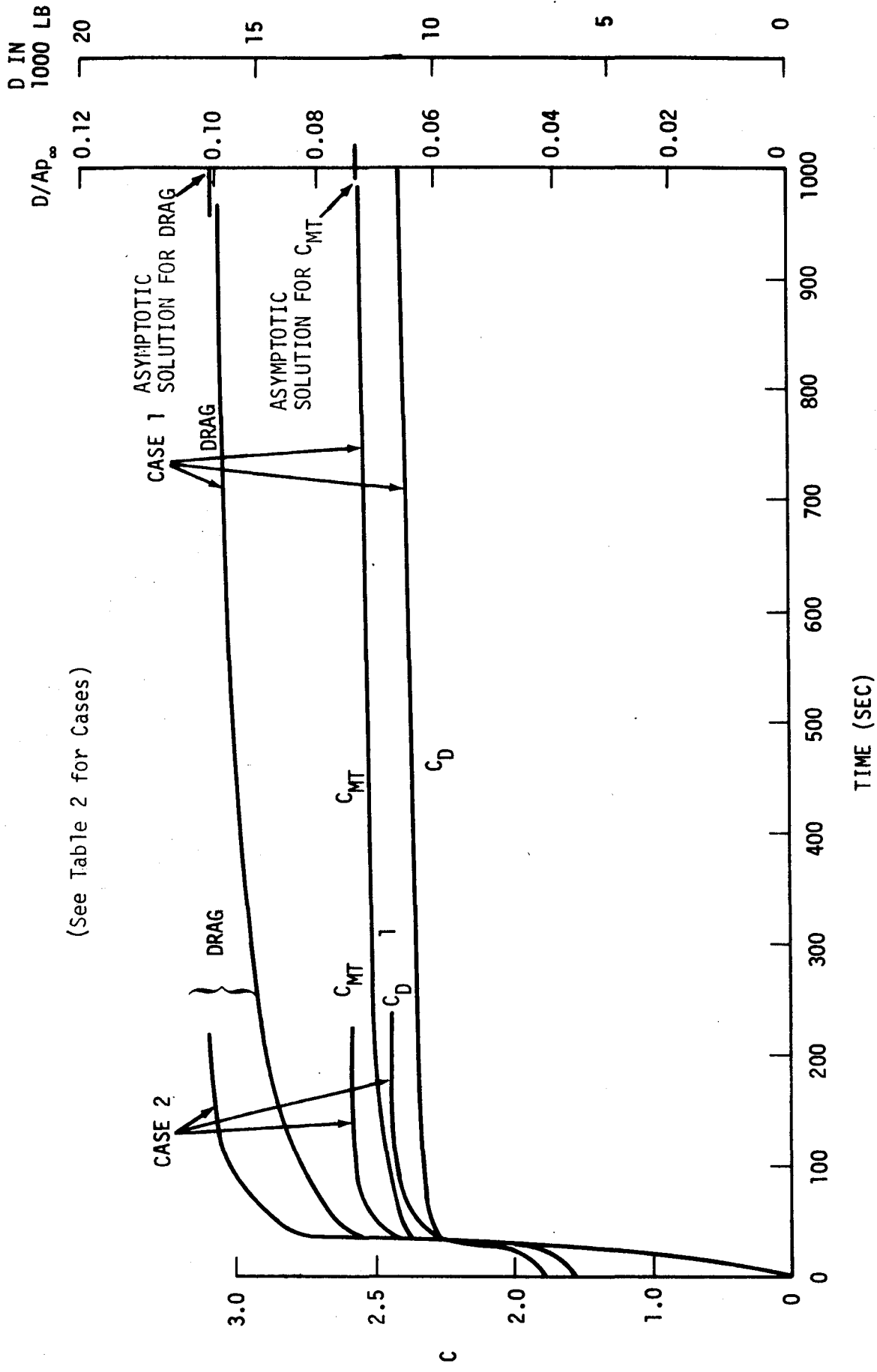


Figure 10. Relative Mach Number as a Function of time for Cases 1, 2, 4, 5, and 6



(See Table 2 for Cases)

Figure 11. Drag, Drag Coefficient, and Momentum Loss Coefficient for Cases 1 and 2

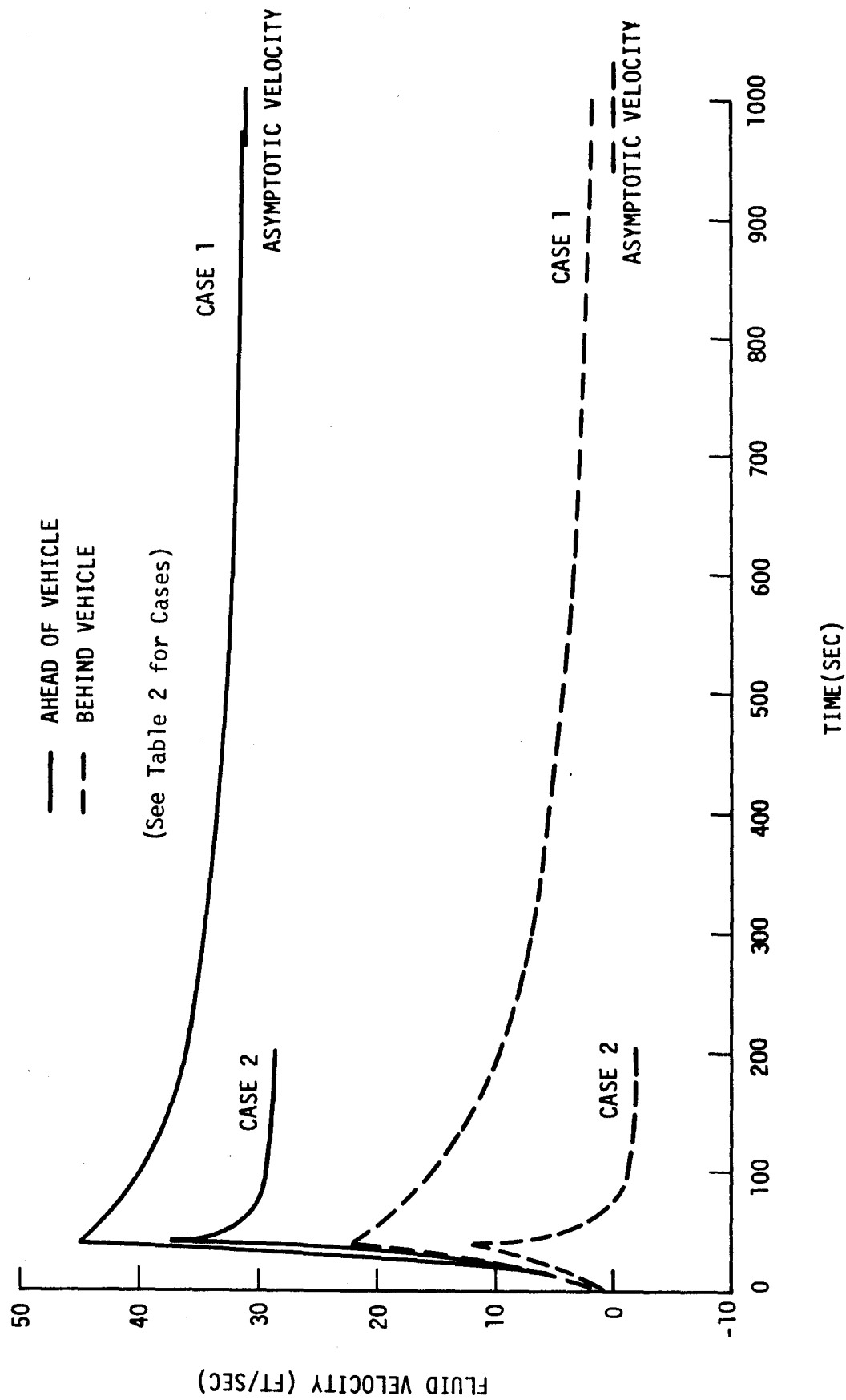


Figure 12. Induced Velocity as a Function of Time for Cases 1 and 2

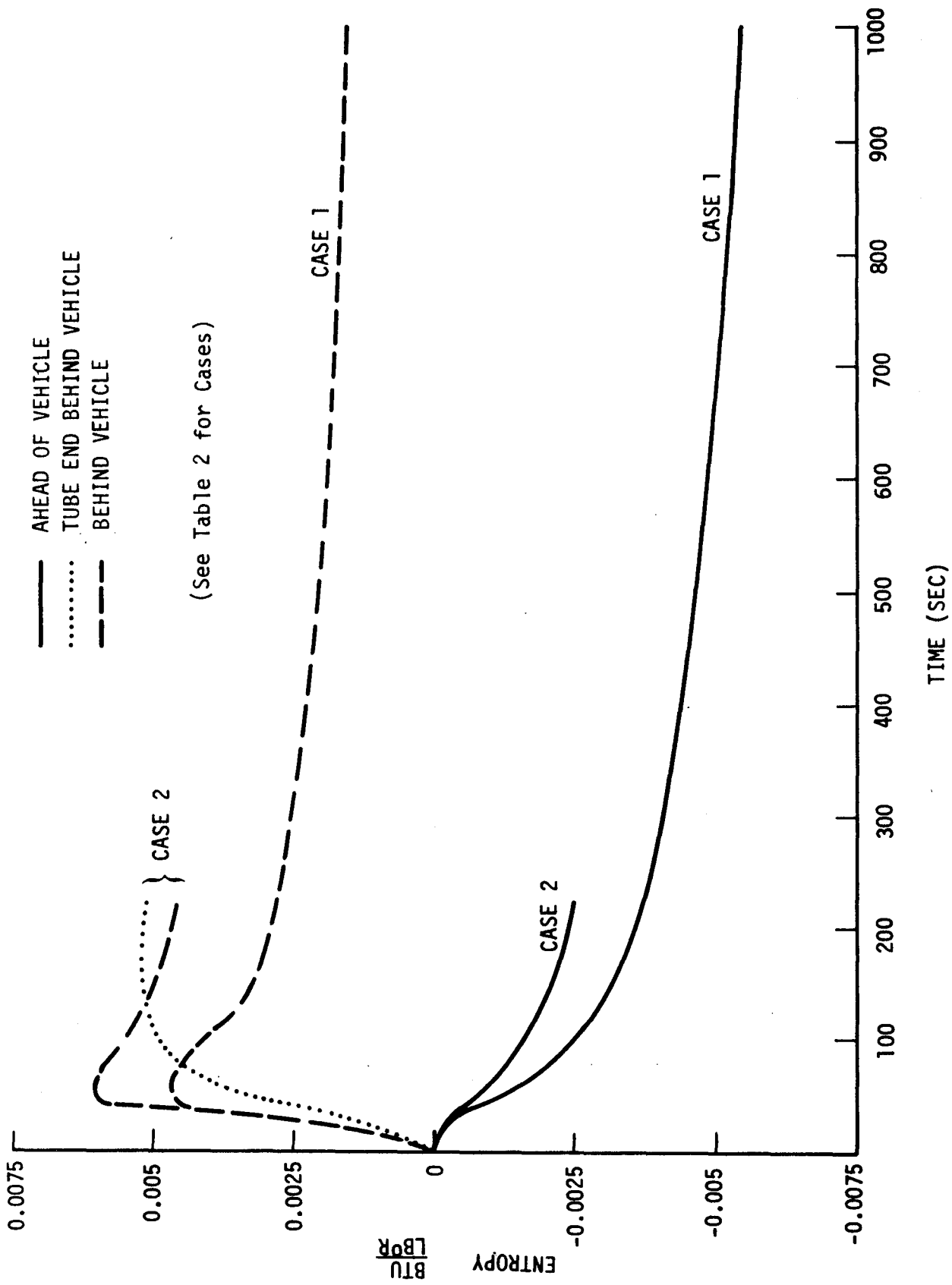


Figure 13. Entropy as a Function of Time for Cases 1 and 2

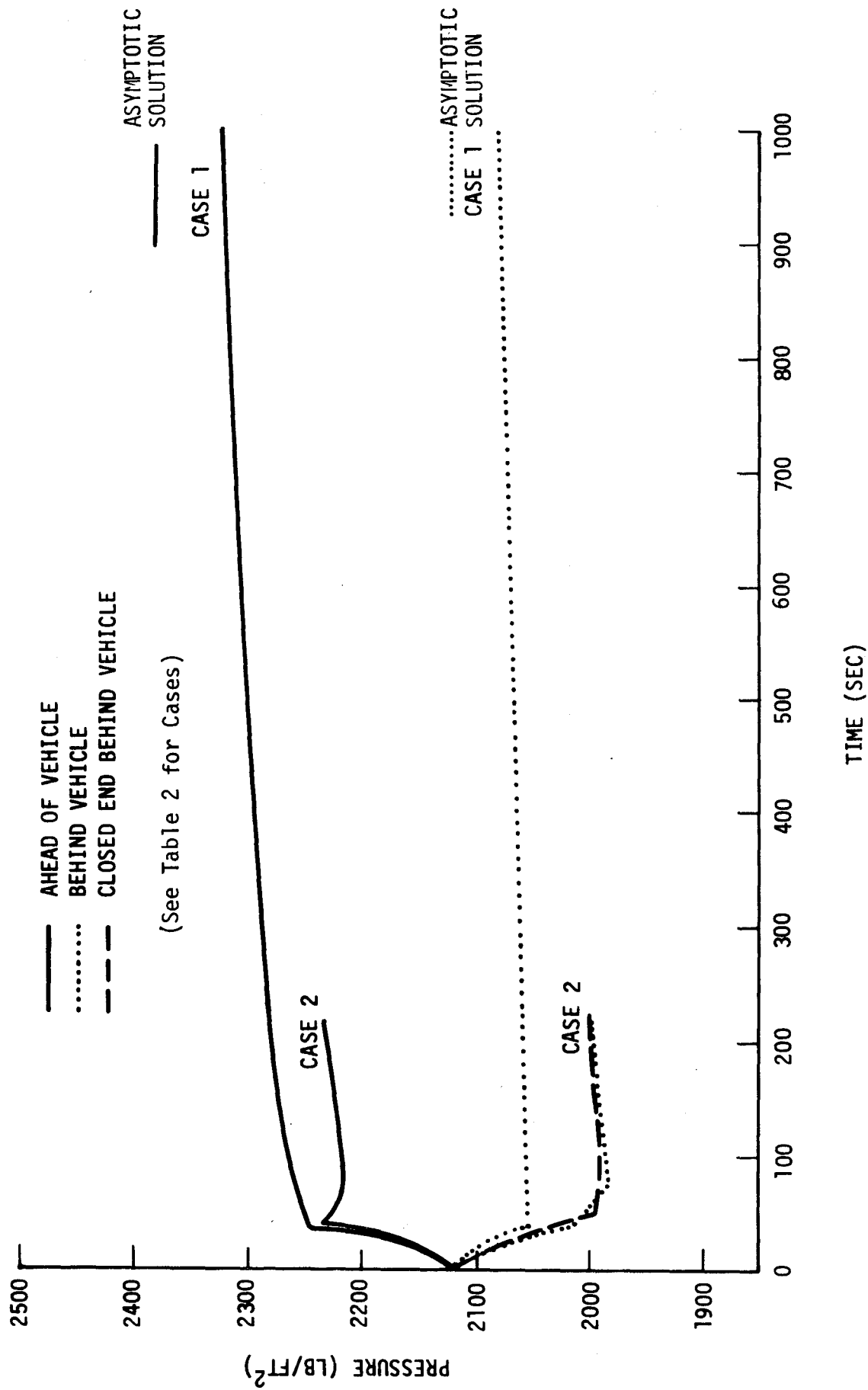


Figure 14. Pressure as a Function of Time for Cases 1 and 2

ASYMPTOTIC SOLUTION

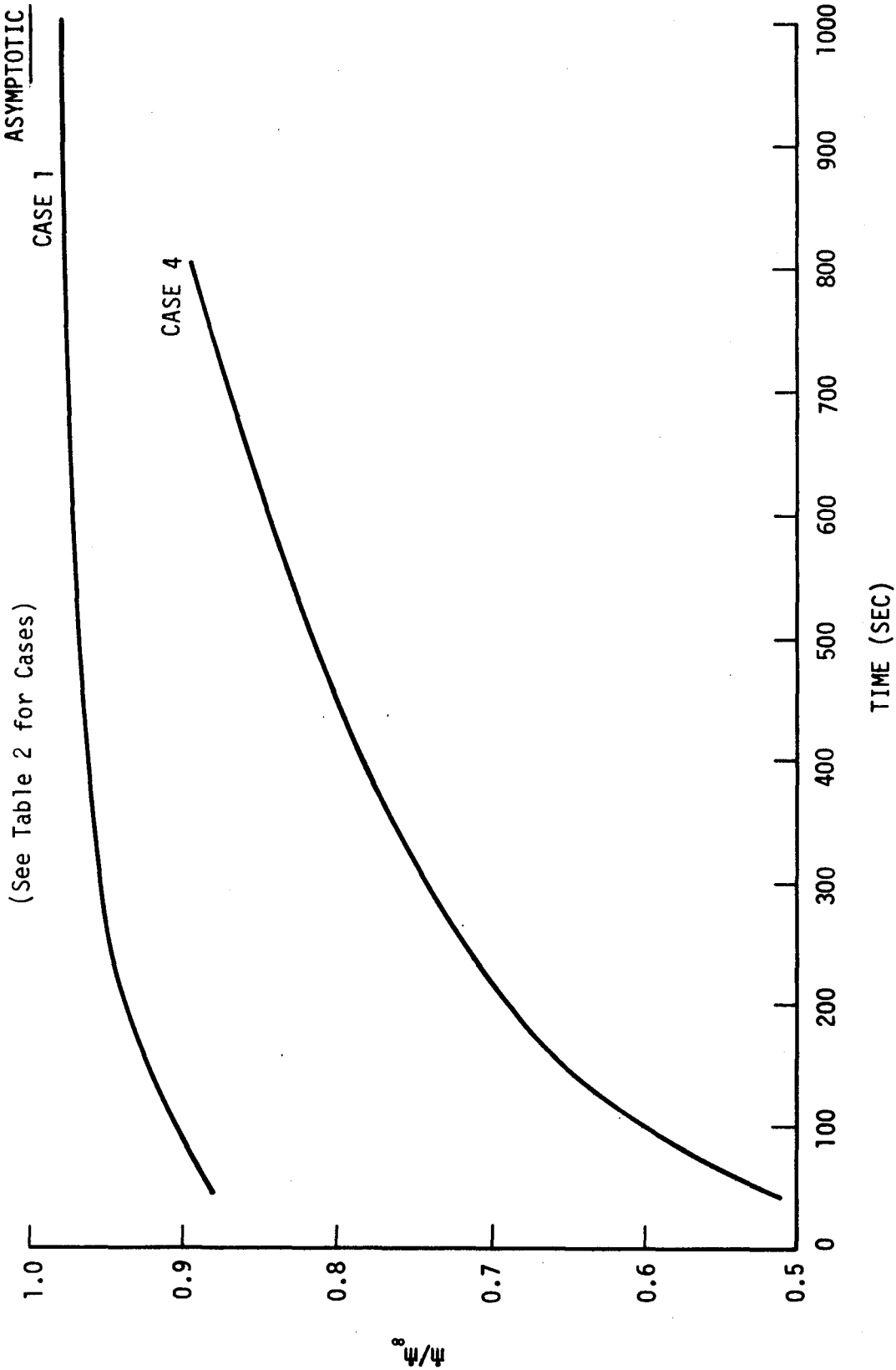


Figure 15. Mass Flow Past the Vehicle Divided by Mass Swept-out by Vehicle for Undisturbed Conditions as a Function of Time for Cases 1 and 4

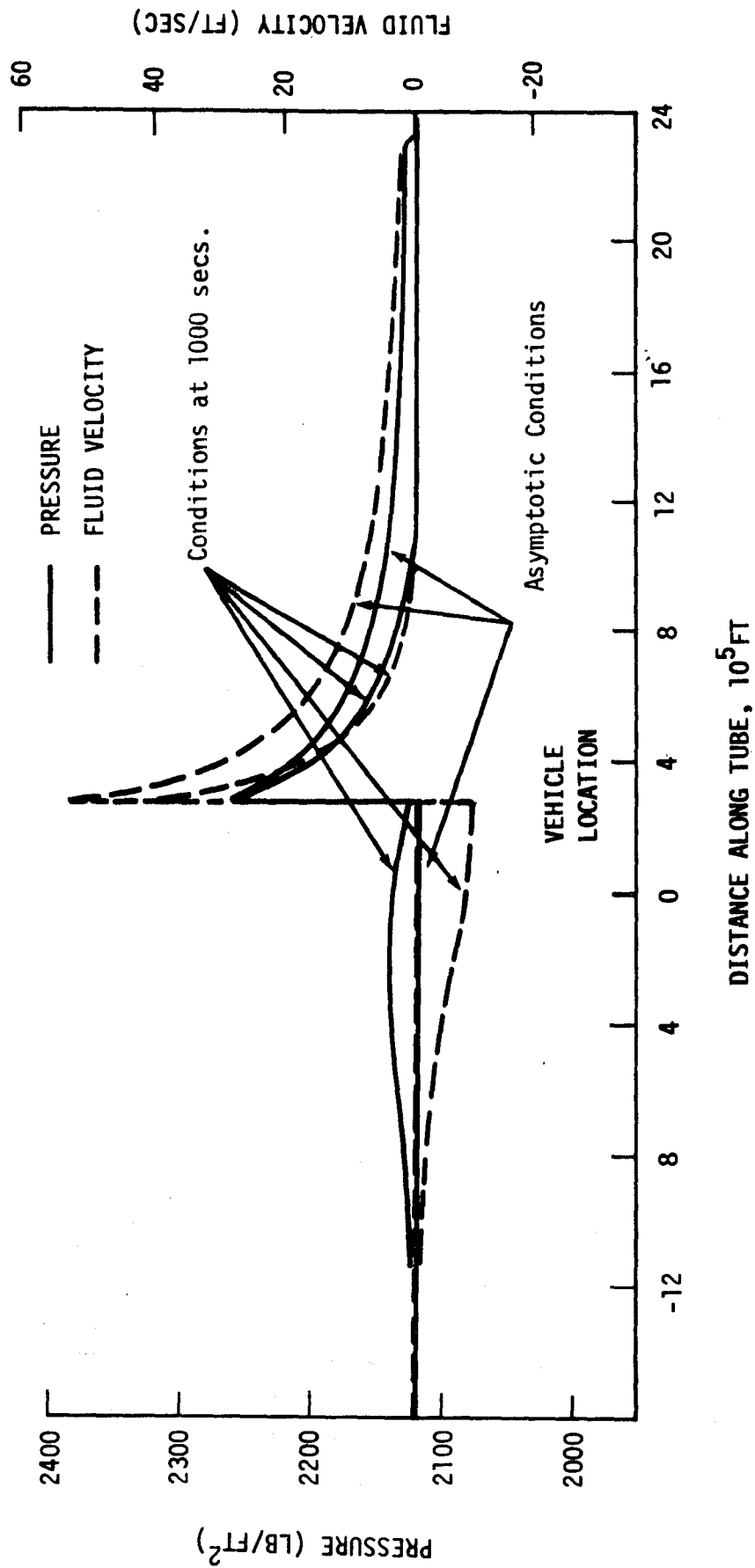


Figure 16. Induced Velocity and Pressure as a Function of Distance Along the Tube at $t = 1000$ seconds, Case 1 (See Table 2) and as given by the asymptotic solution.

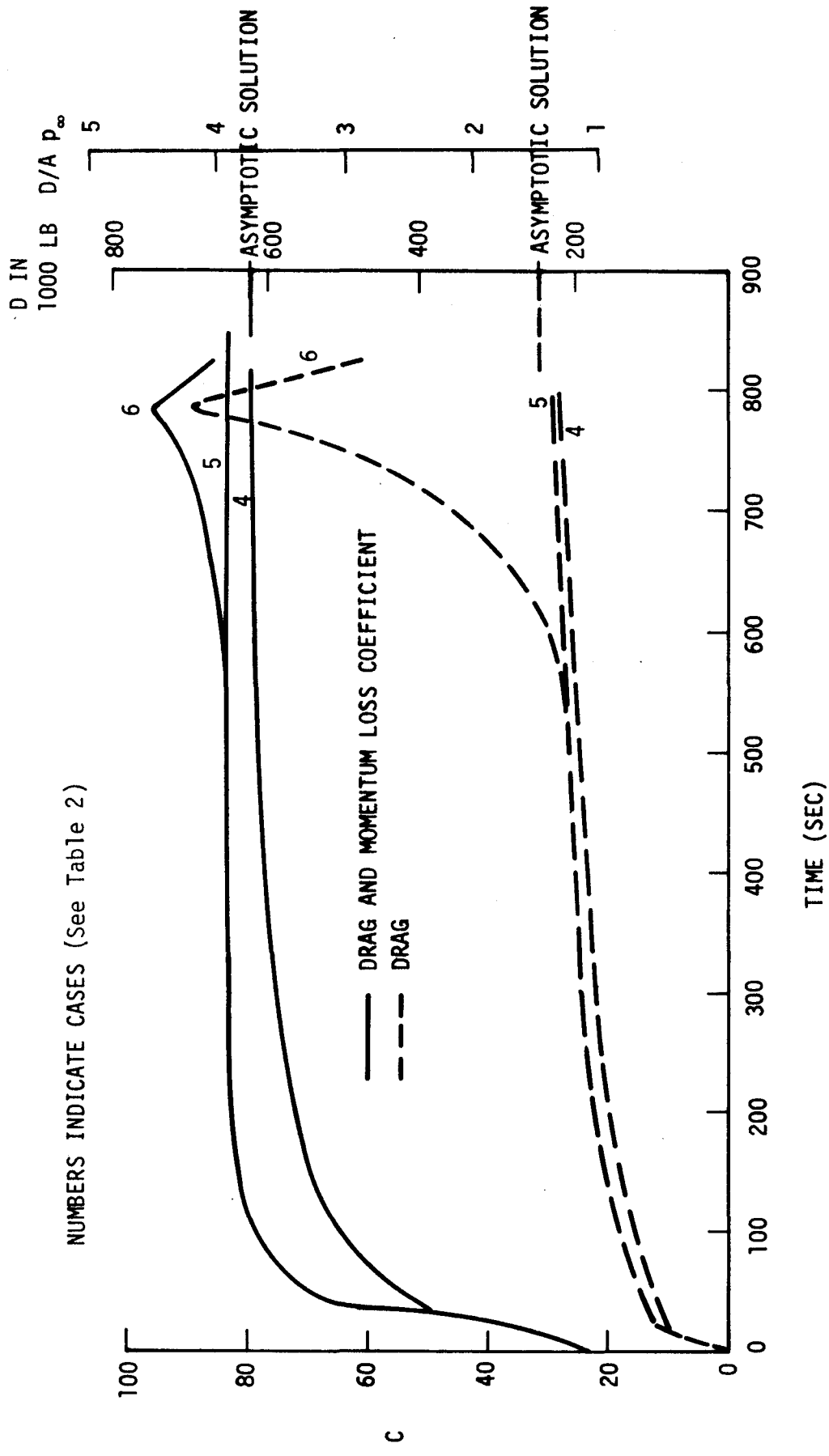


Figure 17. Drag, Drag Coefficient, and Momentum Loss Coefficient as a Function of Time for Cases 4, 5, and 6

NUMBERS INDICATE CASES (See Table 2)

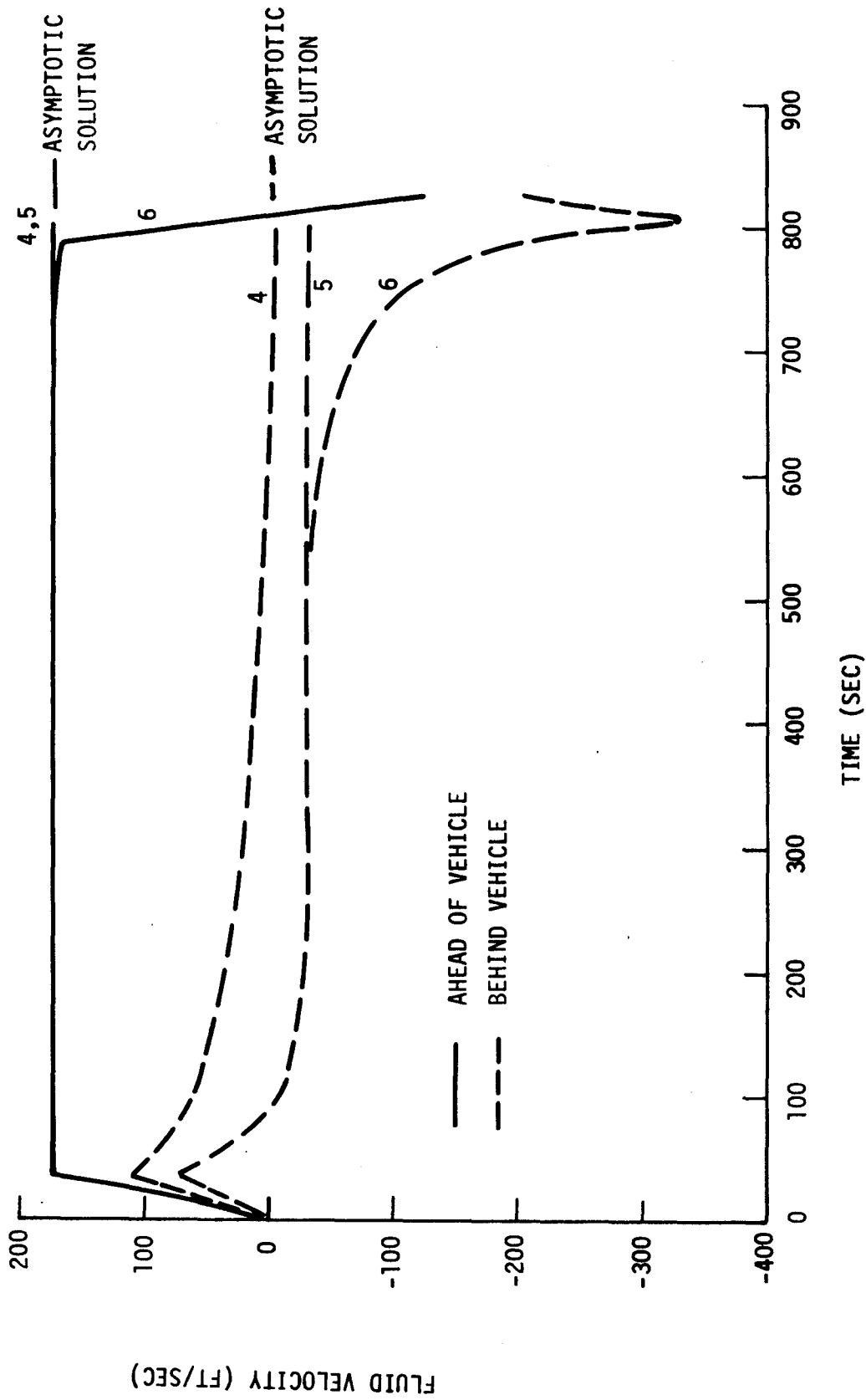


Figure 18. Induced Velocity as a Function of Time for Cases 4, 5, and 6

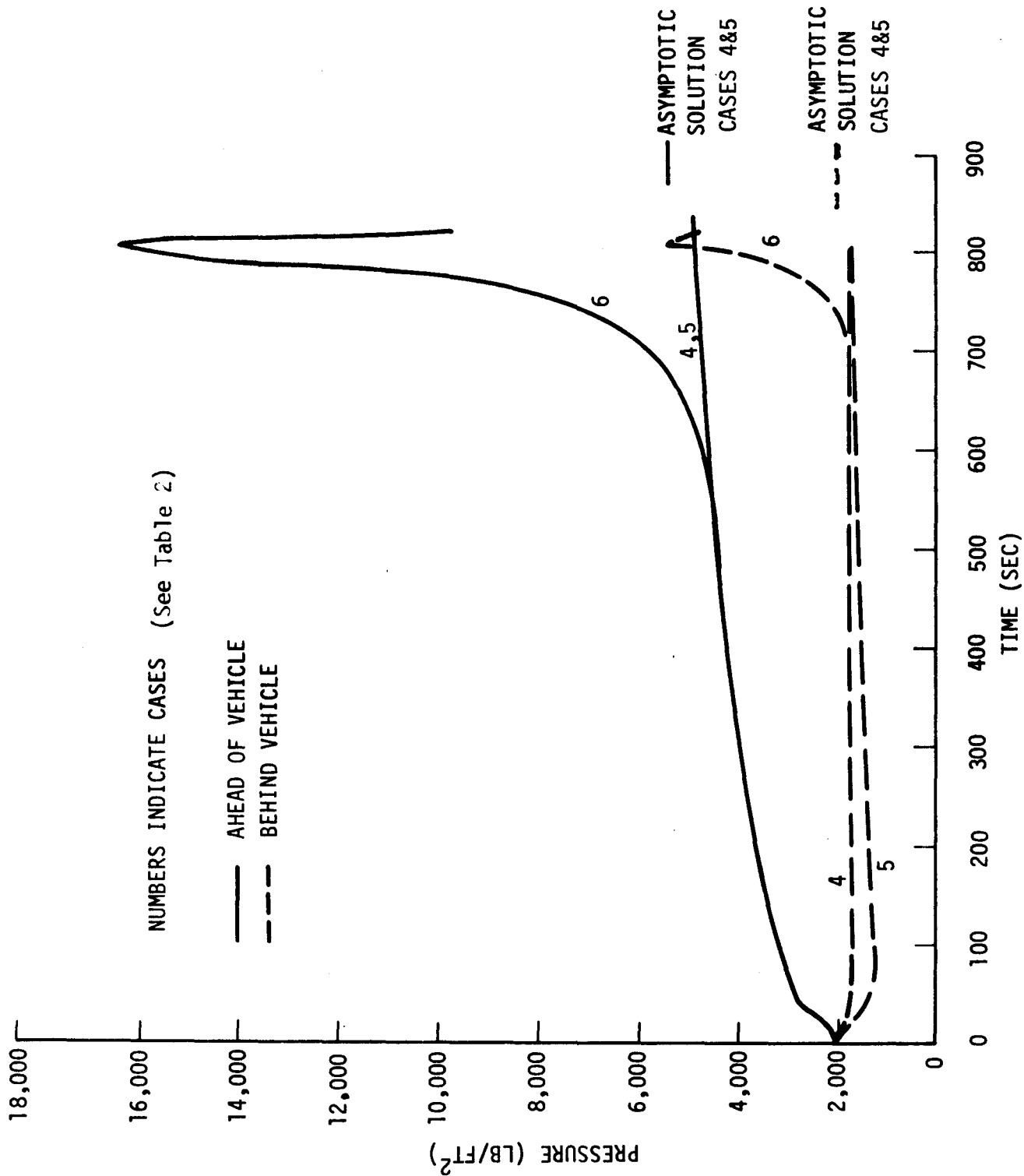


Figure 20. Pressure as a Function of Time for Cases 4, 5, and 6

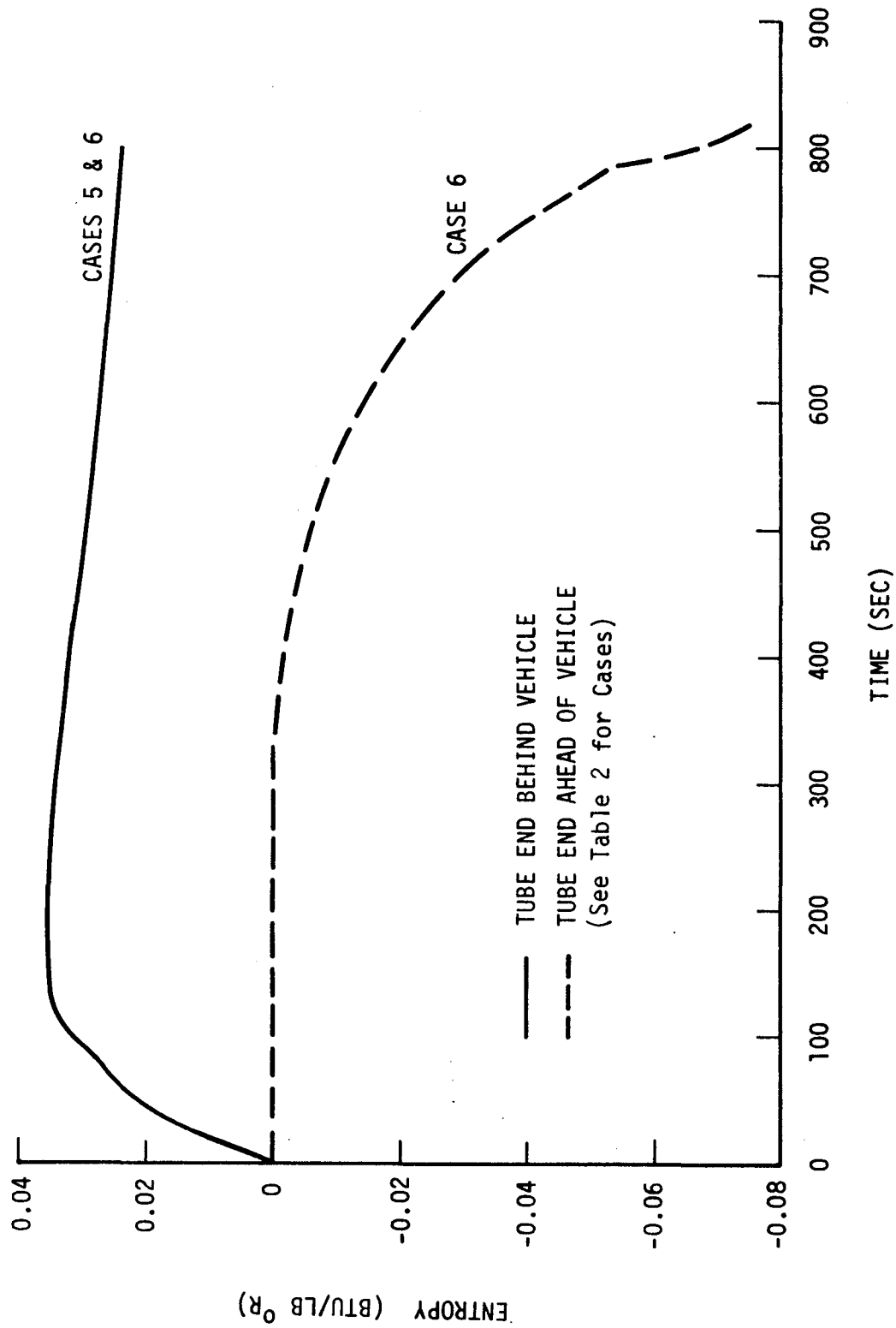


Figure 21. Entropy at the Closed Tube Ends In Front of and Behind the Vehicle as a Function of Time

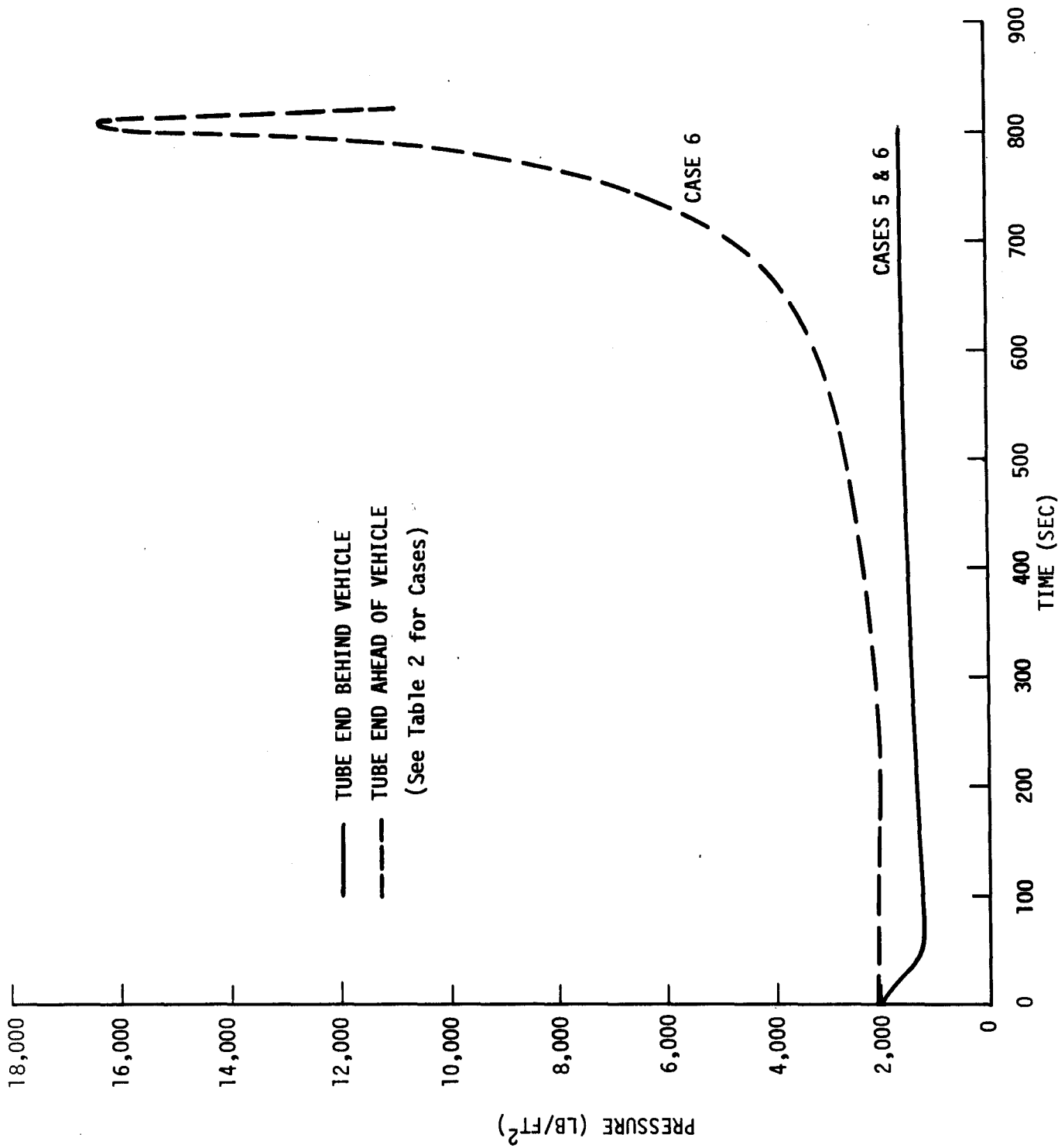


Figure 22. Pressure of the Closed Tube Ends In Front of and Behind the Vehicle as a Function of Time

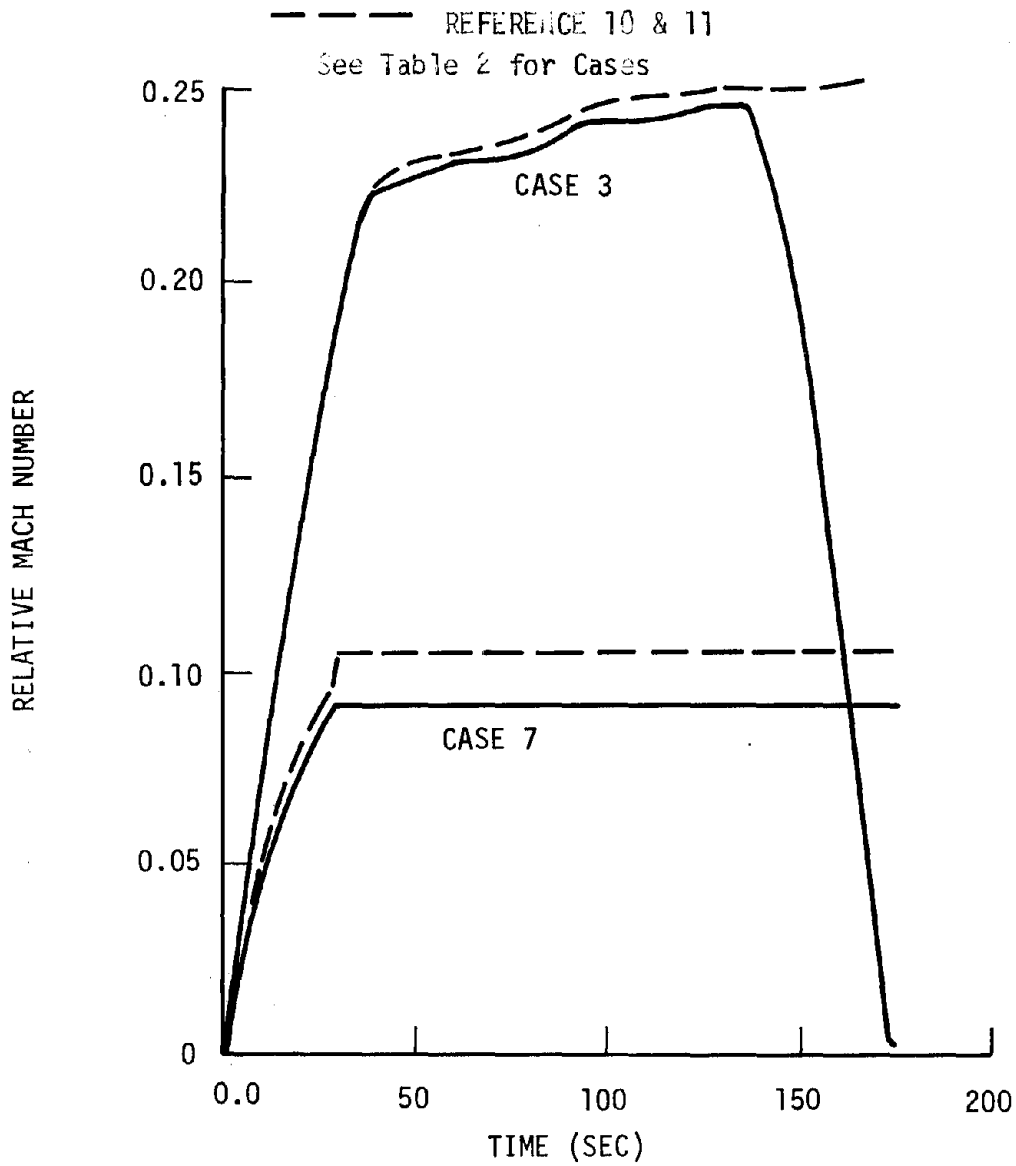


Figure 23. Relative Mach Number as a Function of Time for Cases 3 and 7

See Table 2 for Cases

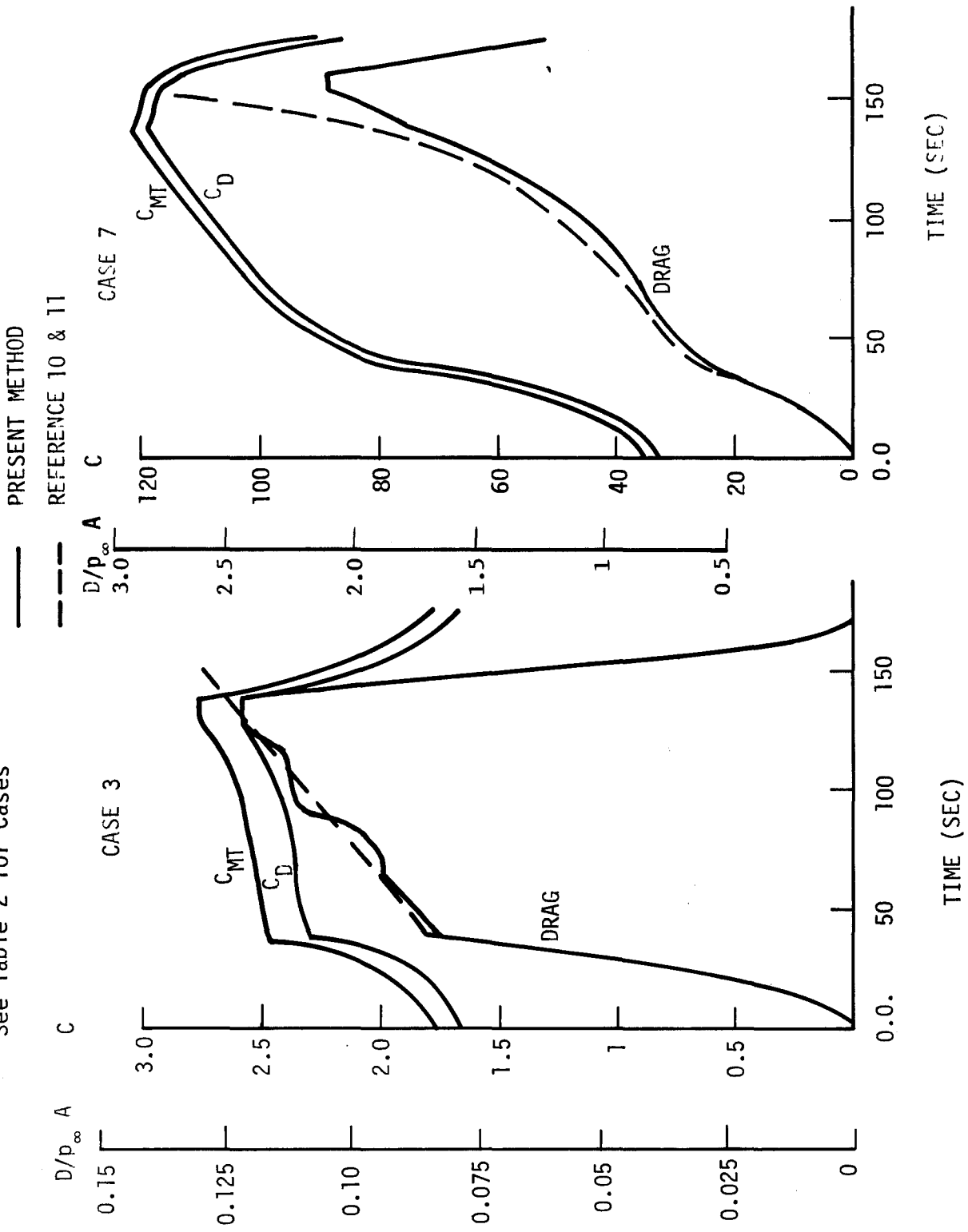


Figure 24. Drag, Drag Coefficient, and Momentum Loss Coefficient as a Function of Time for Cases 3 and 7

See Table 2
for Cases

- AHEAD OF VEHICLE
- BEHIND VEHICLE
- - - REFERENCE 10 & 11 AHEAD OF AND BEHIND VEHICLE

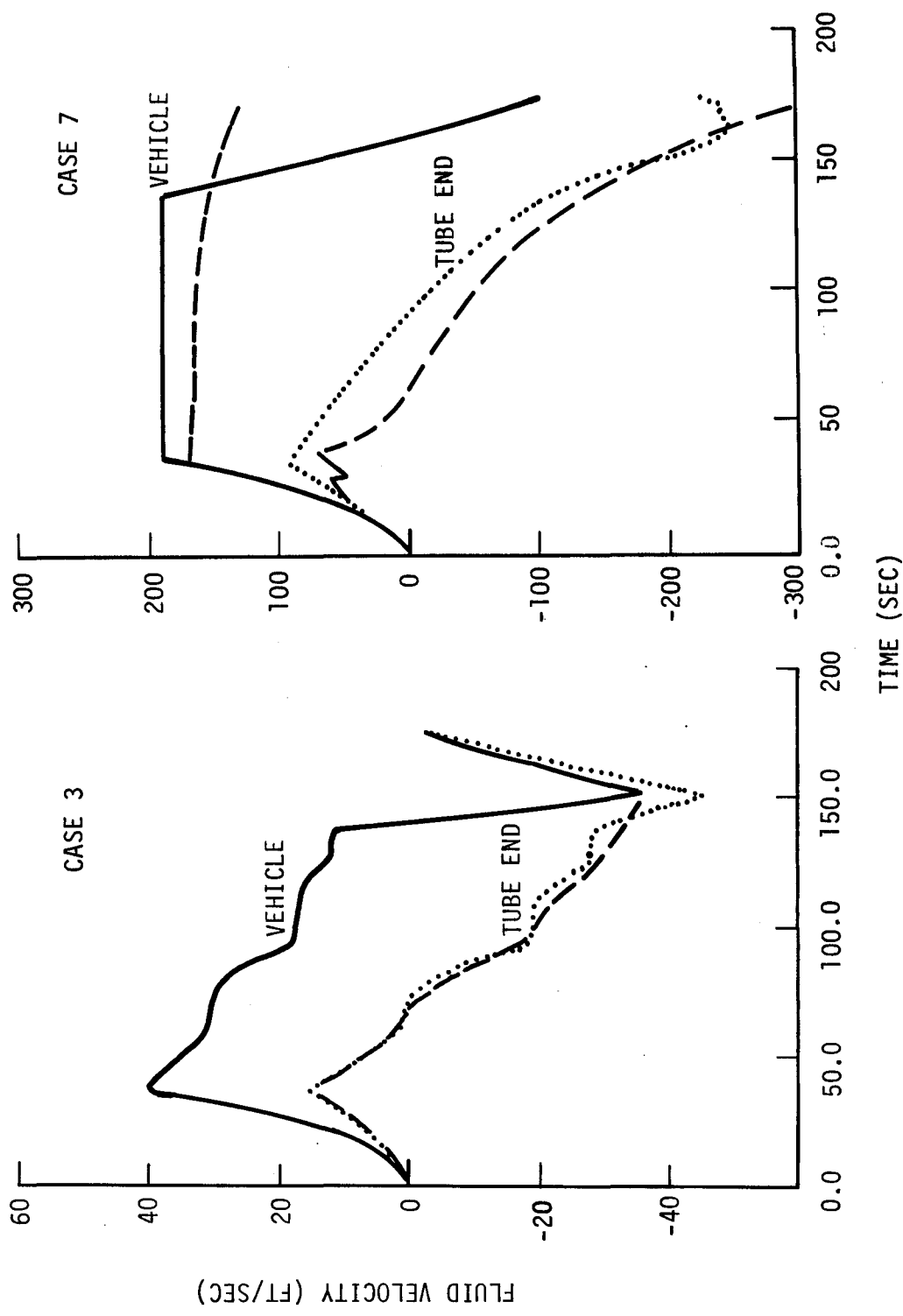


Figure 25. Induced Velocity as a Function of Time for Cases 3 and 7

REFERENCE 10 & 11 AHEAD OF VEHICLE
 AHEAD OF VEHICLE
 BEHIND VEHICLE

.....
 ———
 - - - - -

See Table 2 for Cases

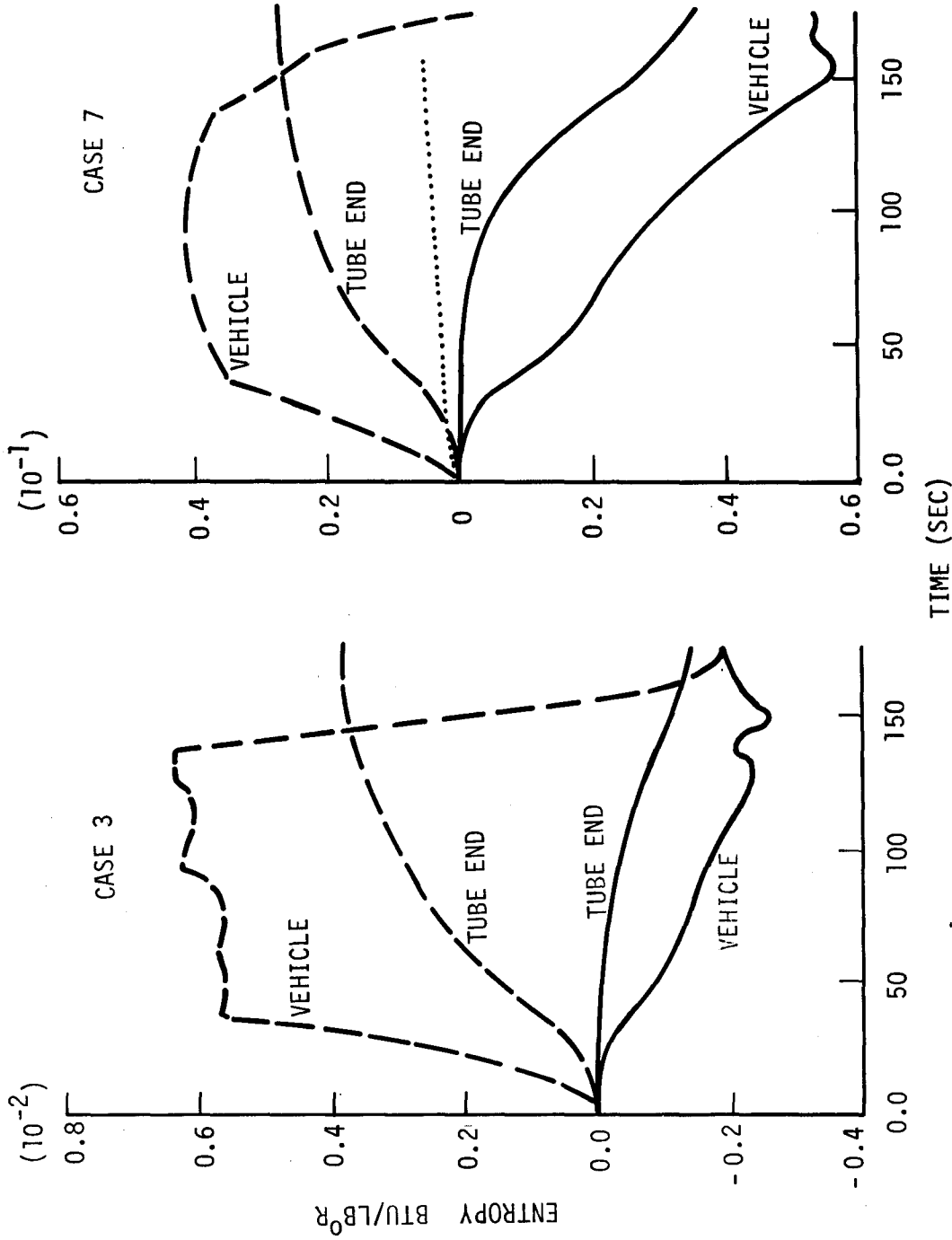


Figure 26. Entropy as a Function of Time for Cases 3 and 7

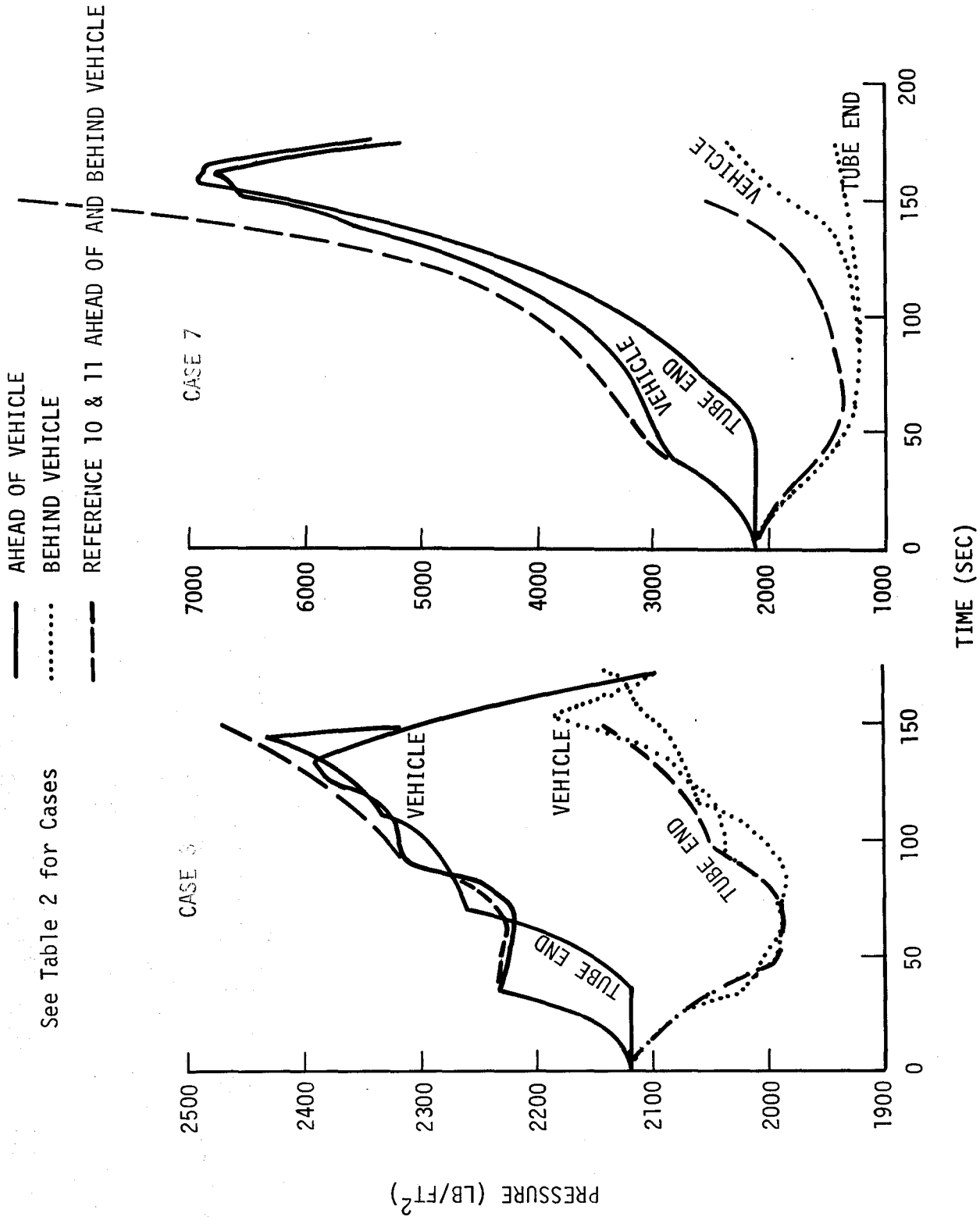


Figure 27. Pressure as a Function of Time for Cases 3 and 7

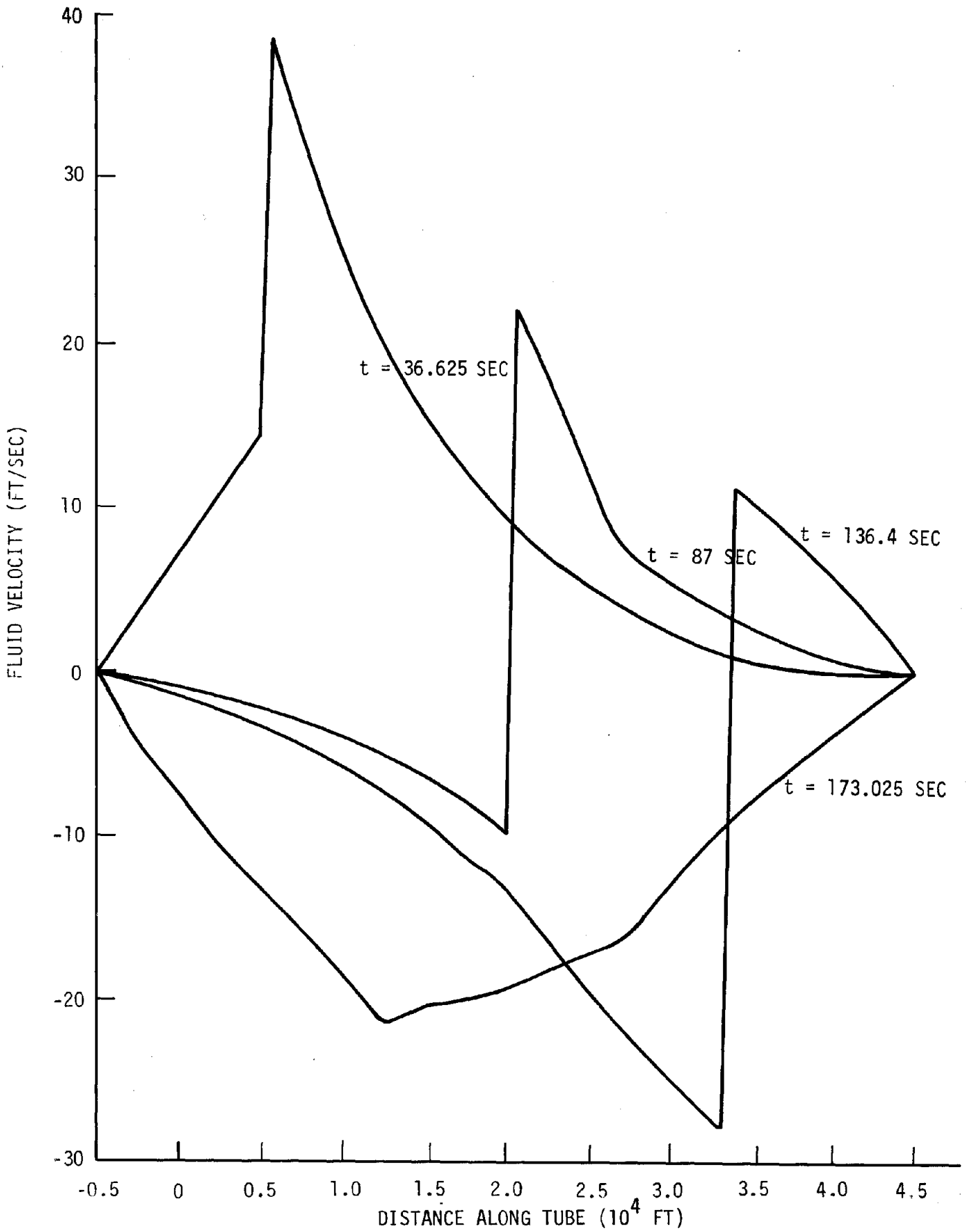


Figure 28. Induced Velocity as a Function of Position Along the Tube for Case 3 (See Table 2)

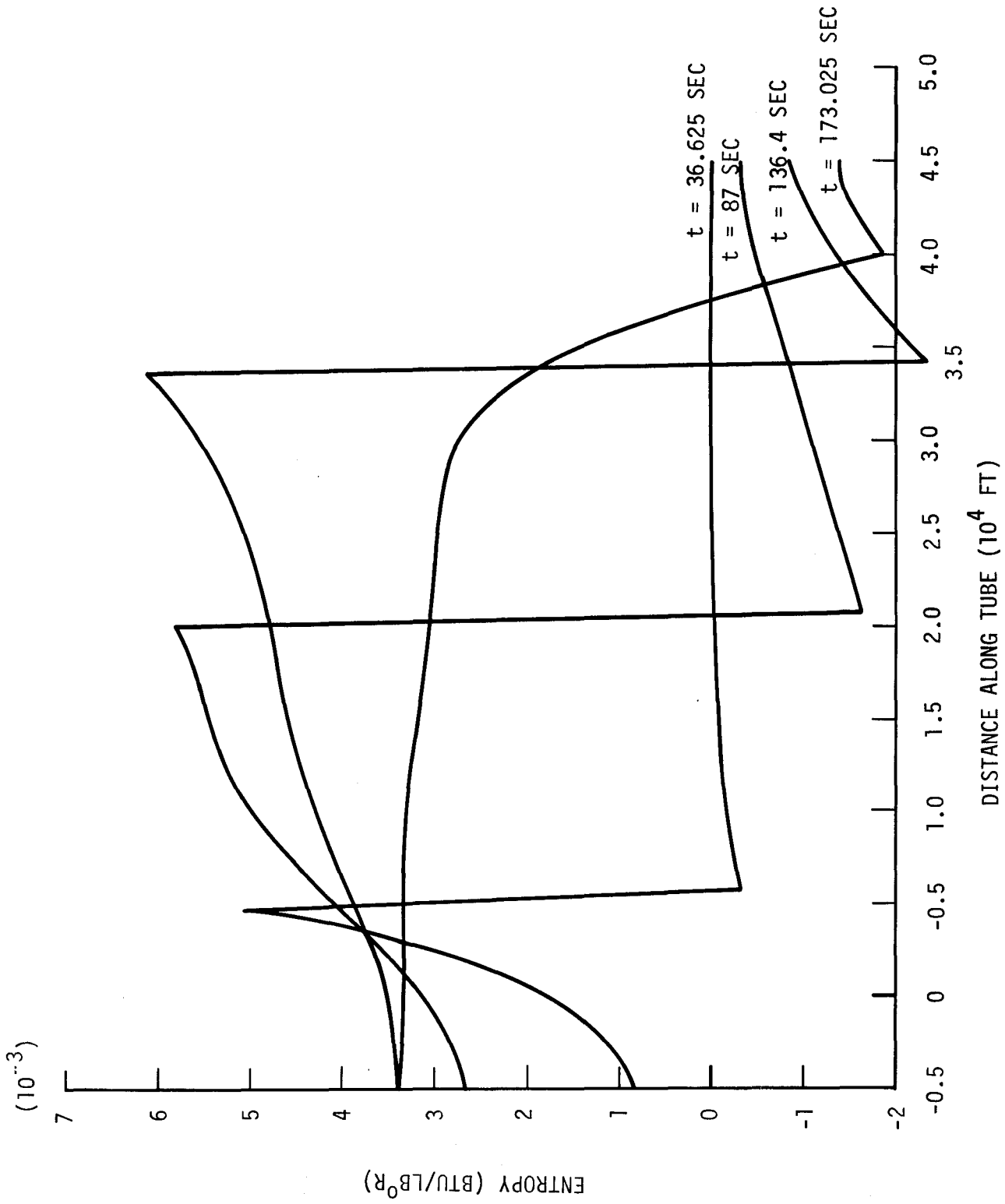
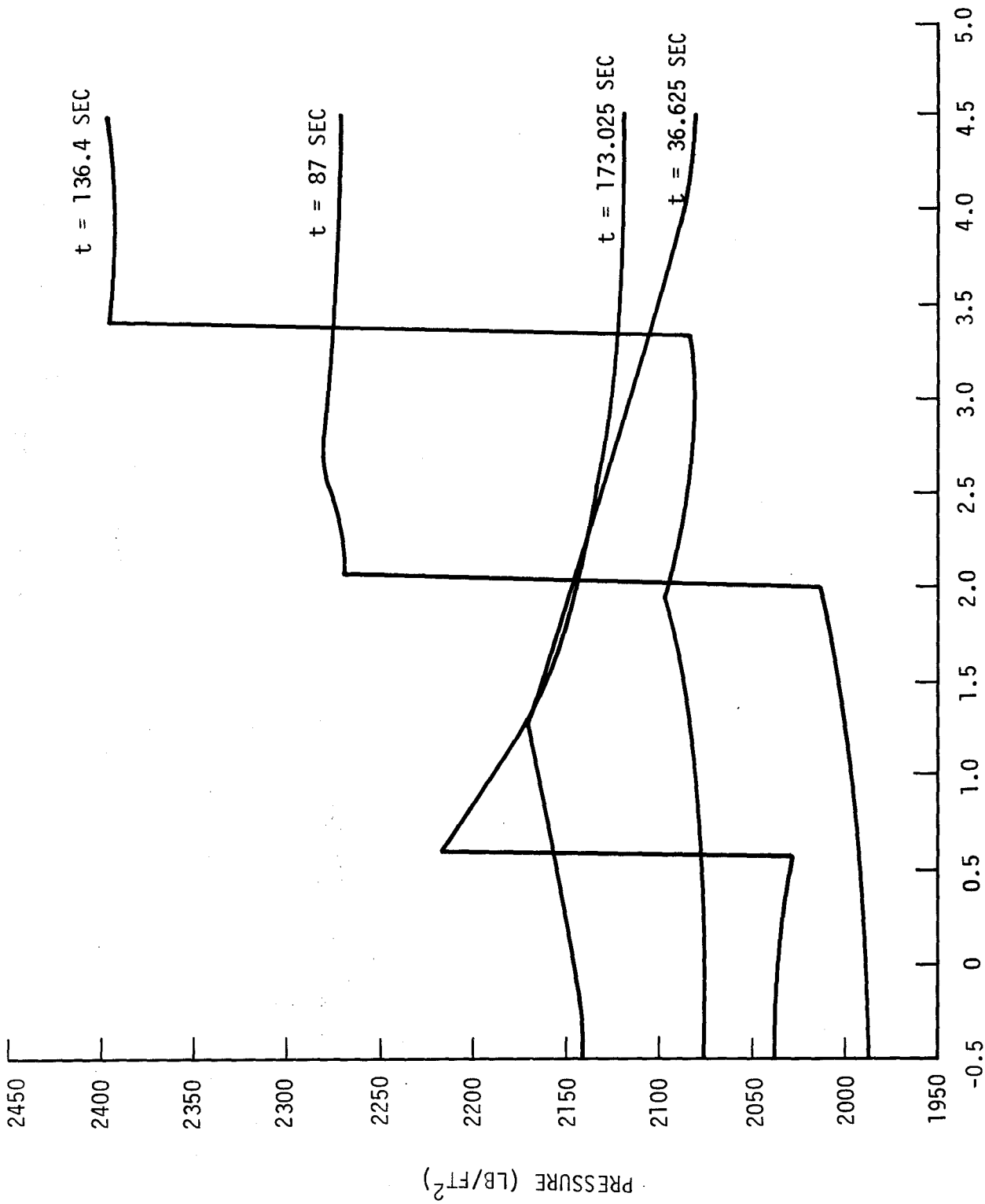


Figure 29. Entropy as a Function of Position Along the Tube for Case 3 (See Table 2)



DISTANCE ALONG TUBE (10⁴ FT)

Figure 30. Pressure as a Function of Position Along the Tube for Case 3 (See Table 2)

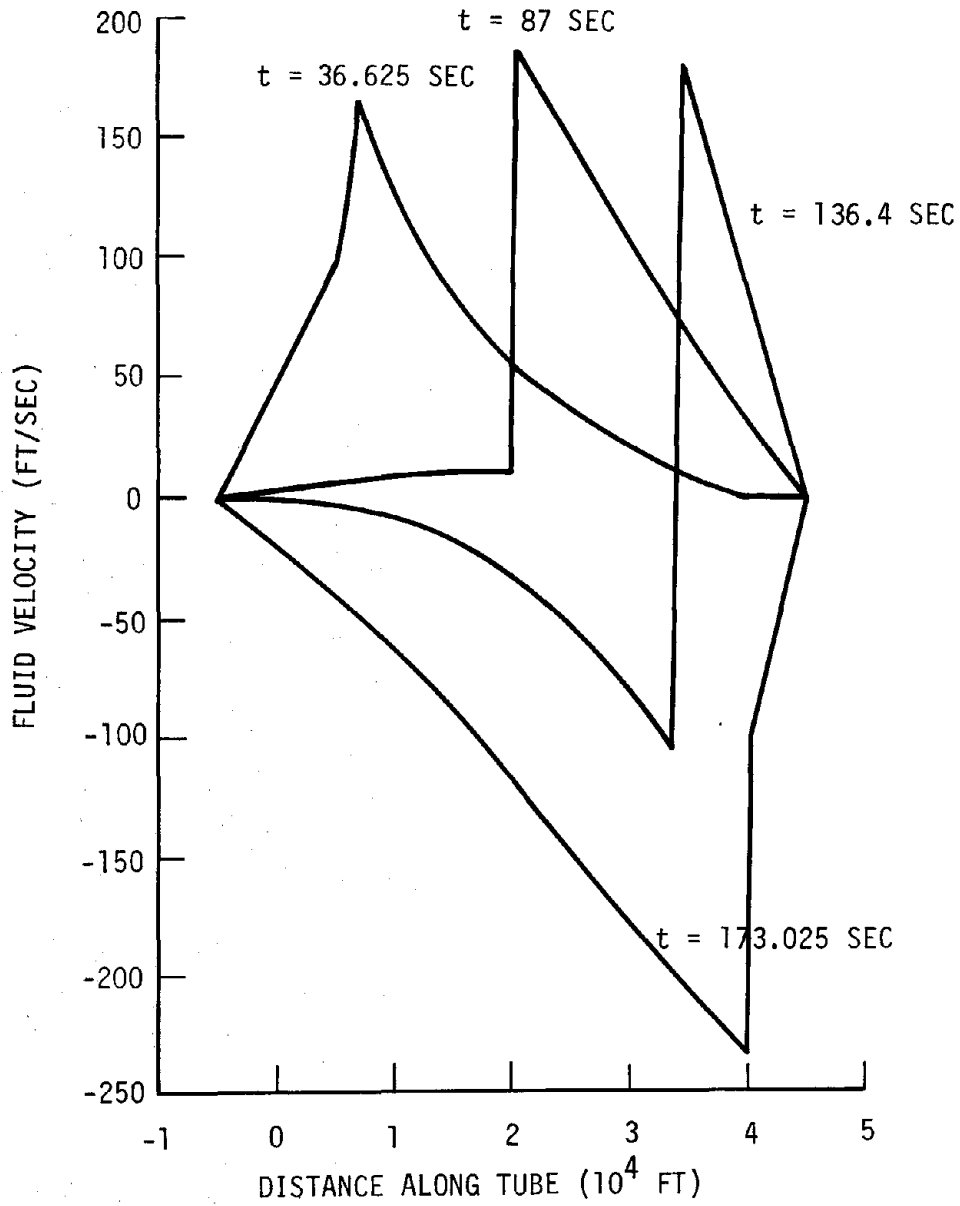


Figure 31. Induced Velocity as a function of Position Along the Tube for Case 7 (See Table 2)

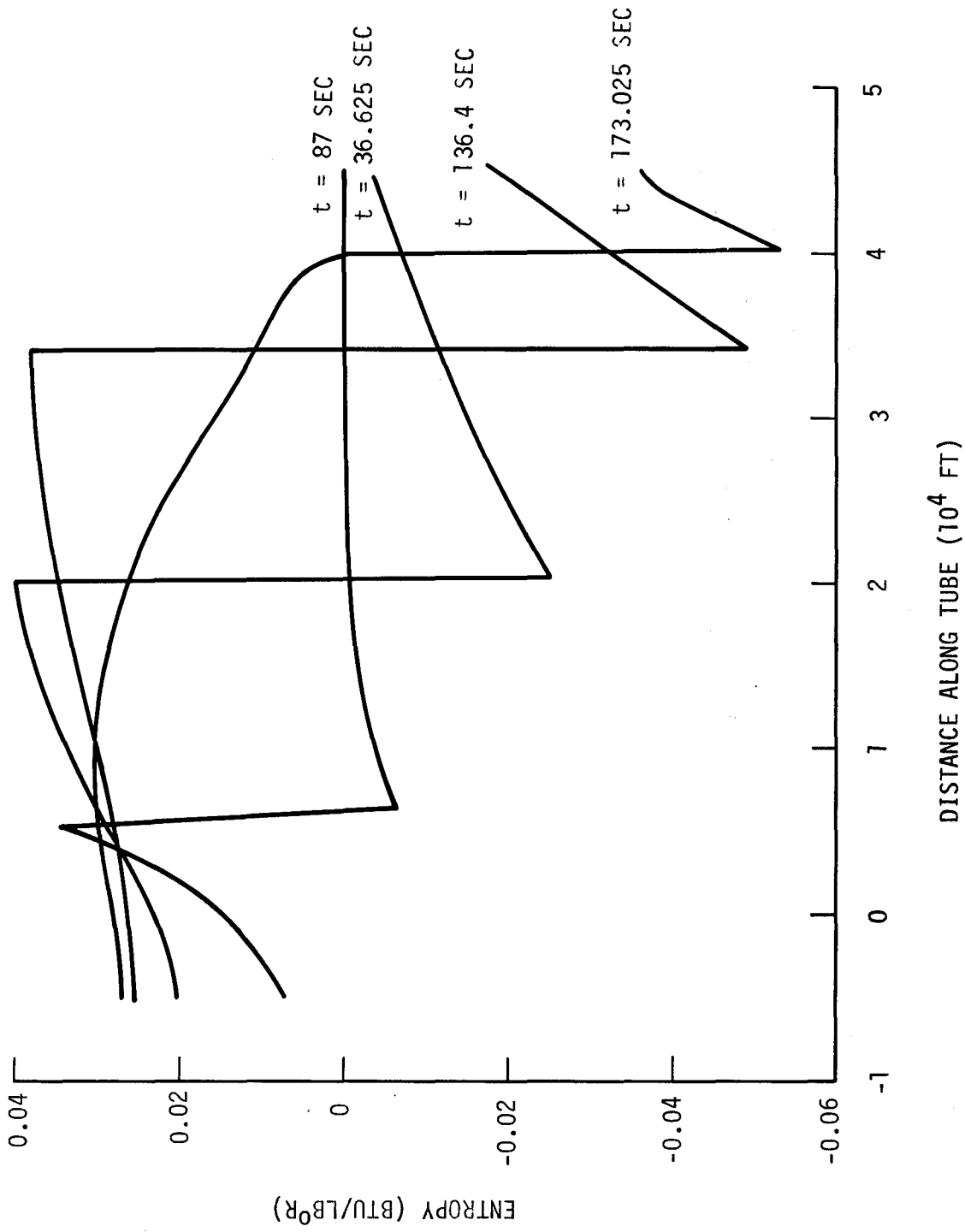


Figure 32. Entropy as a Function of Position Along the Tube for Case 7 (See Table 2)

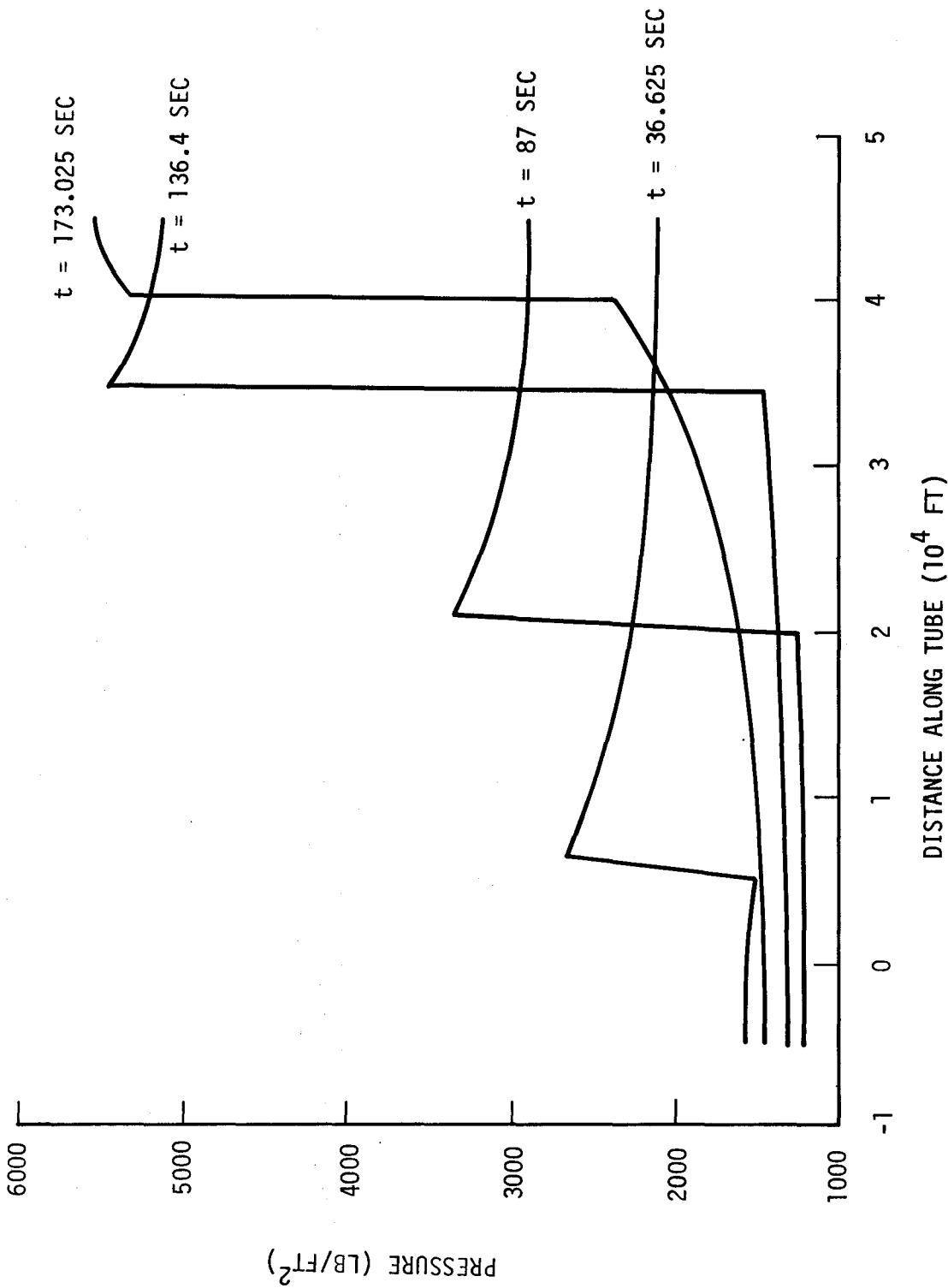


Figure 33. Pressure as a Function of Position
 Along the Tube for Case 7
 (See Table 2)

Cases 1 and 4 were selected in order to assess the aerodynamic effects of both a high and low blockage ratio vehicle starting and traveling through a tube which is long enough so that there is no effect from the ends of the tube within the region affected by the vehicle. The blockage ratios were selected so that choking would not occur for the low blockage ratio vehicle and would occur for the high blockage ratio vehicle. The results presented here for the choked and unchoked flow configurations should be characteristic of these configurations, but calculations of a greater number of cases would be needed to confirm this expectation. The first and most obvious conclusion is that the high blockage ratio vehicle causes a much larger far flowfield effect than the low blockage ratio vehicle. As the blockage ratio and momentum loss coefficient of the vehicle decrease, the far flowfield effects are decreased and for sufficiently low blockage ratio the momentum loss coefficient and drag are too small to cause a far flowfield. Previous results, Reference 4 and 5, had shown that two simple solutions could be obtained to the far flowfield problem which were applicable soon after the start of vehicle travel and after a long time of vehicle travel at constant speed in a long tube. For high blockage ratio vehicles, the drag force on the vehicle is considerably larger for the long time solution than for the short time solution. One of the purposes of Cases 1 and 4 is to determine how long a distance of vehicle travel and how long a tube is required to approach these long time solutions. It is important to determine whether this is likely to occur in tube lengths of practical interest since the flowfield will then become steady and additional steady flow calculations will not have to be made for longer two lengths, and to use the asymptotic long time solutions as check cases against which to validate the numerical calculations. Both the short and the long time solutions can be used to check the numerical calculations, but the long time solutions are considered to provide a more rigorous criterion. The equations used in the numerical solution are very similar to those used in obtaining the short time solutions, namely, the one dimensional unsteady inviscid wave equations. In the numerical solutions, the viscous terms are also included but these are sufficiently small so that they will not have a significant effect over short times and distances. The long time solutions are dominated by the viscous terms. For the numerical solutions to approach these long time solutions the integrated effects of the viscous terms must be correctly included.

Figures 8 and 9 show the position and velocity of the vehicle within the tube as a function of time for all cases. The location of the ends of the tube is also specified in Figure 8. Figure 10 shows the relative Mach number and Figure 11 the drag coefficient, drag, and momentum loss coefficient for Case 1 as the vehicle travels along the tube. The asymptotic value for the momentum loss coefficient from the long time solutions is also shown. For Case 1 the relative Mach number is always below the choking value. Figures 12 through 14 show the velocity, entropy, and pressure both directly ahead of and behind the vehicle. The significance of the velocity and pressure is obvious, but the significance of the entropy is possibly more obscure. The changes in entropy show the effects of the irreversible friction and heat transfer processes. If these processes were not included in the calculation, then the entropy would be constant. Friction alone would only increase the entropy while heat transfer can have either effect. Heat flow to the walls will cause a decrease in entropy while heat addition to the fluid will cause an increase in entropy. Ahead of the vehicle the entropy decreases because of the heat flow to the walls from the fluid which has been heated by compression. The entropy increases in flowing about the vehicle because of the friction and separation losses. The entropy of the fluid which was originally behind the vehicle is increased both because of the friction from the walls and heat addition to cool expanded fluid. The fact that the entropy decreases in front of the vehicle shows that the heat transfer effect is more important than the friction and demonstrates the importance of including the heat transfer term. The velocity and pressure shown in Figures 12 and 14 appear to be approaching the asymptotic limits but have not yet reached them. The asymptotic long time solution gives the rather surprising result that there is no disturbance behind the vehicle. Another condition of the asymptotic solution is that the flow is steady in vehicle fixed coordinates and the mass flowing past the vehicle must be equal to the rate at which mass would be swept out by the vehicle moving into the undisturbed fluid. This result is shown in Figure 15. Initially, the mass flux past the vehicle, \dot{m} , is considerably less than that being swept out by the vehicle, \dot{m}_∞ , but it increases so that by 1000 seconds the two values are approaching each other.

The velocity and pressure along the tube after the vehicle has traveled for a time of 1000 seconds are shown in Figure 16 along with the predictions of the asymptotic solutions. The condition for the asymptotic solutions to be valid is that the waves have propagated a sufficient distance so that they have been attenuated by friction and heat transfer and have become of negligible strength. The frictional compression in front of the vehicle should not have a distinct front but be asymptotic to the undisturbed conditions at infinity. Figure 16 shows that these wave fronts have not yet dissipated completely and have not propagated far enough ahead to establish the asymptotic solutions. Behind the vehicle, the conditions are also considerably different. The disturbance introduced by the passage of the train has not yet had time to attenuate to the asymptotic solution. The calculations have not been carried out to larger values of time because of the time and cost of doing so and because the tube lengths involved are considerably beyond those considered to be of practical interest.

The conclusion based on this comparison of the numerical and asymptotic solutions is that the numerical solutions show a definite tendency to approach the values given by the asymptotic solutions. However, whether they will reach precisely these values cannot be determined without carrying out the calculations further. The agreement shown so far indicates a reasonable assurance of the accuracy of the numerical calculations, but not enough to give a precise evaluation of the error that may have been introduced in the numerical integration process.

Figures 8 through 10, 15, and 17 through 22 shown similar results for the large blockage ratio configuration. In this case, the magnitude of the far flowfield disturbance is much larger; the induced velocity in front of the vehicle is greater than half the velocity of the vehicle itself. The relative Mach number reaches the choking value during the acceleration of the vehicle and is constant after that. Because of the greater strength of the waves created by this vehicle, they do not attenuate to as small a value as those caused by the lower blockage ratio vehicle and conditions do not approach as near to those given by the asymptotic solution in the time available. The velocity behind the vehicle has actually somewhat overshoot the asymptotic value and gone negative. Without actually carrying out the calculations to much larger values of

time it is impossible to predict that the velocity will return to zero. However, considering the larger positive values of velocities that exist further behind the lower blockage ratio vehicle shown in Figure 16 it is not unreasonable that they will do so.

Case 2 and 5 are similar to 1 and 4 except that a closed end has been placed behind the starting position of the vehicle at a distance of 2000 feet. The results for these cases are also shown in Figures 8 through 22. This closed end causes a reduction in the velocity and pressure behind the vehicle. Both the drag coefficient, the drag of the vehicle and momentum loss coefficient are increased. However, the increase in drag is much larger for the choked vehicle. Another obvious difference between the choked and unchoked vehicle is that the closed tube end placed behind the choked vehicle has no effect on the flow in front of the vehicle which is exactly the same as it was for the previous case in which there was no closed end behind the vehicle. The increased drag is caused by the lower pressure behind the vehicle. For the unchoked vehicle, the changes in conditions behind the vehicle cause corresponding changes in front of the vehicle. Because the vehicle drag coefficient is only dependent on the relative Mach number of the fluid in front of the vehicle, the pressure difference across the vehicle must remain approximately constant and the reduced pressures behind the vehicle cause a corresponding reduction in the pressure in front of the vehicle. This reduced pressure in front of the vehicle does cause some increase in relative Mach number which causes some increase in the drag coefficient but not nearly as much as for the choked vehicle. The discontinuous nature of the conditions behind the vehicle and at the tube end is caused by the waves generated by the initial acceleration of the vehicle reflecting between the tube end and the vehicle. These waves are attenuated by their reflections from the vehicle and by friction and heat transfer. One might expect that as the vehicle travels further from the closed tube end, the effect of this end would be reduced and that the results for these cases would approach those of the previous case and the long time asymptotic solutions. This does appear to be the case but at the maximum time calculated the two solutions are different. These calculations cover a distance of about 50 miles of vehicle travel and about 200 miles of wave travel in both directions from the initial vehicle position if not reflected by a tube end.

Case 6 is similar to Case 5 except that a closed end has been placed in the tube at 232,000 feet from the vehicle starting point. The vehicle is decelerated to stop 2000 feet from the end of the tube giving a vehicle travel of 230,000 feet or 43.6 miles. The solution is identical to Case 5 up to 215 seconds when the waves first reach the far end of the tube. However, these waves must be reflected and travel back to the vehicle before there can be any change in conditions at the vehicle. These first waves are relatively weak having been attenuated by their travel through the tube and it is not until about 500 seconds when the vehicle has traveled for 140,000 feet that conditions on the front of the vehicle begin to change noticeably from the previous case. However, as the vehicle continues to approach the end of the tube, the pressure between the vehicle and the end of the tube rises rapidly as well as the vehicle drag coefficient, drag, and momentum loss coefficient. The fluid which has been pushed ahead of the vehicle as it traveled down the tube is now trapped between the vehicle and the tube end and must escape around the vehicle. There is still a high pressure in front of the vehicle even after it has come to a stop. The fluid in front of the vehicle is now flowing towards the vehicle and around it to escape to the low pressure regions behind the train. The pressure is still large enough even at the time the vehicle has stopped so that the flow about the vehicle is still choked and the relative Mach number is still at the critical value. While the calculation has not been continued, this situation should not last more than 5 or 10 seconds since the length of this high pressure region is only 2000 feet. For a high blockage vehicle of this type, the high pressure cushion formed between the vehicle and the end of the tube is an effective braking means which should prevent the vehicle from running into the end of the tube but which could lead to very high decelerations.

Cases 3 and 7 are for shorter tube lengths and were calculated particularly to provide check cases to be compared with similar cases being calculated by MITRE. These two cases are for a high and low blockage ratio vehicle in a 50,000 foot tube which starts and stops 5000 feet from the ends of the tube. The calculation already discussed for long tubes show that for a tube of this length the viscous force never becomes dominant and the flowfield chiefly depends on inviscid effects. The results are shown in Figures 23 through 33. For the

low blockage ratio, Case 3, the flow never chokes and the pressure between the end of the tube and the vehicle never becomes particularly high. By the time the vehicle is brought to rest, the pressure difference across the vehicle has become quite small. For the high blockage ratio, Case 7, the flow is choked over much of the trajectory and remains choked up until the time at which the vehicle has been brought to rest. In this case the pressure in front of the vehicle becomes quite high as it approaches the far end of the tube. Plots of velocity, entropy, and pressure are shown along the tube at several values of time corresponding to the end of vehicle acceleration, near the middle of vehicle travel, at the beginning of vehicle deceleration, and at the time the vehicle has been brought to rest. These plots are shown in Figures 28 through 33.

In all cases, the vehicle drag has been shown for a vehicle in a 10 foot diameter tube and an initial pressure of one atmosphere. These results can be relatively easily applied to different tube diameters and initial pressures. In addition to the drag, the quantity

$$\frac{D}{p_{\infty} A}$$

is also shown. This quantity should be approximately the same for tubes of different size or initial pressure and can be used to calculate these different conditions.

Case 3 and Case 7 were selected in conjunction with the MITRE Corp. in order to compare the two sets of calculations. These calculations are made using the same basic equations and boundary conditions but integrating these equations using a different method. The present method integrates the partial differential equations along the characteristic directions. MITRE performs the integration by the method of characteristics only in the region near the vehicle and uses a fixed mesh integration in the region far from the vehicle. Both methods of integrating these equations are accepted ones and should give correct results.

A comparison of the near flow field for Case 3 has been made and MITRE's results are in agreement with those presented in Figure 3. The near flow field results for Case 7 have not been compared in detail but Figure 23 shows a higher choking Mach number for the MITRE result. The inclusion of the relative motion between the vehicle and the wall in the MITRE solution would be expected to cause an increased choking Mach number, although this has not been verified in detail.

Comparisons of far flow field results are shown in Figures 23 through 27 between the present calculations and those obtained by MITRE for Cases 3 and 7, References 10 and 11. The results near the end of the run differ because the MITRE vehicle does not decelerate to a stop before the end of the tube. The results for Case 3 are in fairly good agreement. For the unchoked conditions the current data shows small scale variations with time not evident in the MITRE results. The MITRE solution might show similar results if a smaller mesh spacing were used. The results for choked conditions (Case 7) show a greater difference. The differences occur after choking conditions have been reached and continue to increase with time of vehicle travel.

For choked flow, Case 7, small discontinuities which occur in the MITRE solutions at the choking point would not be expected in the actual flow and can probably be disregarded in the comparison. MITRE's results show a lower induced velocity ahead of the vehicle which is consistent with the higher choking Mach number; however, they show a higher drag and pressure in front of the vehicle which is inconsistent with the higher choking Mach number. Consistent with the higher pressure and lower induced velocity, MITRE's results also give a higher temperature and entropy in front of the vehicle. A comparison of entropy provides an insight into the viscous effects predicted by the two methods since, if the flow were inviscid, the entropy change would be zero everywhere. The MITRE results show a small increase in entropy in front of the vehicle while present results show a decrease. The effect of heat transfer to the wall dominates the friction effect resulting in the decrease in entropy. The increase in temperature is smaller than would occur in the isentropic case. This result is thought to be correct since it is consistent with the asymptotic solutions.

These differences are demonstrated by comparing properties in front of the vehicle after the vehicle has traveled for 136 seconds at which time the vehicle in the present study begins to decelerate.

	<u>MITRE Result</u>	<u>Present Study</u>
$p - p_{\infty}$, lbs/ft ²	4245	3363
$T - T_{\infty}$, °F	210	38
$S - S_{\infty}$	+ 0.004	- 0.0486
$\frac{D}{p_{\infty} A}$	1.985	1.792

The main differences are in the temperature and entropy with smaller differences in the pressure and drag. From the results at 136 seconds it is difficult to assess the magnitude of these differences at long vehicle travel times (e.g. 1000 seconds). The differences in temperature show that the heat transfer to the wall in the present calculation is considerably larger than in the MITRE calculation. The pressure and drag in the MITRE calculation are higher than the present calculation which correspond to the higher temperature and entropy but is opposite to what would be expected from the higher critical Mach number.

In summary, the initial effects are primarily inviscid. Although there is a slight variation in critical Mach number for the choked condition, the comparisons show good agreement after a short time of travel for both choked and unchoked flow. As the time of travel increases viscous effects become more dominant particularly for the choked flow case. The differences in viscous effects are more pronounced for temperature and entropy than for pressure and drag.

4. CONCLUSIONS

The conclusions resulting from the study can be summarized as follows:

1. If the flow about a vehicle is choked, changes behind the vehicle do not influence conditions in front of the vehicle and a qualitatively different flow field from the unchoked condition is created.
2. The locations of the ends of the tube have a pronounced influence on the flow field conditions within the tube. This effect is most pronounced for high blockage vehicles which cause a strong far flow field.
3. When the vehicle is approaching a closed tube end located in front of the vehicle the flow field effects are more pronounced than when it is leaving a closed tube end located behind the vehicle.
4. The distance of vehicle travel required to reach the steady state asymptotic conditions are in excess of $2(10^4)$ tube diameters (45 miles in a 10 foot diameter tube) for the cases calculated. Since the flow mechanisms and the relative importance of the viscous and inviscid terms is continuously changing as the vehicle travels along the tube, calculations and experiments in short tubes are not adequate to determine flow conditions in long tubes.
5. The analytic, long time, asymptotic flow solutions (References 4 and 5) provides an upper limit of the drag for the cases calculated. The actual vehicle drag has approached to within 10% of this value for a distance of vehicle travel of 10.7 miles for the low blockage vehicle of Case 1 and for a distance of vehicle travel of 43.5 miles for the higher blockage vehicle of Case 4. The relative Mach numbers and drag coefficients approach their asymptotic values more quickly but the pressure and vehicle drag lags behind.
6. The time and distance of vehicle travel required to approach the steady asymptotic values increases with vehicle blockage ratio. This result was predicted in Reference 4 and 5 and is born out by two cases presented in this calculation.
7. The viscous effects become increasingly more important as the distance of vehicle travel increases and do not reach their full magnitude until the conditions approach their asymptotic values.
8. Comparisons of results from the present study and a similar study of MITRE (References 10 and 11) show good agreement for unchoked flow about the vehicle (Case 3). However, for choked flow about the model (Case 7) differences occur

which increase with distance of vehicle travel. These differences appear to be caused by variations in the critical Mach number and the magnitude of the viscous effects predicted by the two methods.

APPENDIX A

NEAR FLOWFIELD

1. FRICTION FLOW IN PASSAGE WITH MOVING WALL

The steady flow of fluid through a passage with heat transfer and friction is a classic problem in gas dynamics. If friction alone is acting, the conditions in the fluid follow the Fanno line and if heat addition alone is acting, the conditions follow a Rayleigh line. In the problem of a vehicle moving through a tube, the situation is complicated by having the surfaces of the vehicle moving with respect to the tube, so that we must consider at least one of these walls to be nonstationary in whatever coordinate system is chosen in which to formulate the problem. Since the tube is very long with respect to the vehicle, it is reasonable to expect at least a quasi-steady flow in the vicinity of the vehicle in a coordinate system fixed with the vehicle if the vehicle's motion is reasonably steady. It has also been shown (Reference 5) that the motion everywhere in the tube is steady in a vehicle fixed coordinate system if the tube is very long and the vehicle has been traveling for a long time at constant velocity. Therefore, the problem of the steady flow of a fluid in an annulus in which one wall is stationary and one moving with respect to the coordinate system is one which is important to the flow about a tube vehicle.

If the compressible flow equations are written in a coordinated system fixed with the vehicle, the results are as follows:

$$\text{Continuity} \quad \frac{1}{\rho} \frac{\partial \rho}{\partial x} + \frac{1}{v} \frac{dv}{dx} = 0 \quad \text{A-1}$$

$$\text{Momentum} \quad \frac{dp}{dx} + \tau_{ww} \frac{1}{A} \frac{dA_{ww}}{dx} + \tau_{vw} \frac{1}{A} \frac{dA_{vw}}{dx} + \rho v \frac{dv}{dx} = 0 \quad \text{A-2}$$

$$\text{Energy} \quad \left(C_p \frac{dT}{dx} + \frac{d}{dx} \frac{v^2}{2} \right) \rho v = \left(\tau_{ww} u_s + q_w \right) \frac{1}{A} \frac{dA_{ww}}{dx} + \frac{q_v}{A} \frac{dA_{vw}}{dx} \quad \text{A-3}$$

$$\text{State} \quad p = \rho RT \quad \text{A-4}$$

A_{ww} and A_{vw} are the tube and vehicle wall surface area and A is the flow cross sectional area. The assumption will be made that there is no heat transfer to the vehicle, $q_v = 0$, since, for steady flow conditions, the vehicle cannot act as a heat source or sink. This condition would have to be modified for a vehicle that dissipated power directly as heat. The friction force on the vehicle does not enter the energy equation A-3, since this friction force is acting on a surface that is stationary with respect to the coordinate system and therefore does no work. The friction force and heat transfer can both be expressed in coefficient form by the relations

$$\tau_{ww} = \frac{1}{2} \rho u |u| C_f \quad A-5$$

$$\tau_{vw} = \frac{1}{2} \rho v |v| C_f \quad A-6$$

$$q_w = \rho |u| C_p (T_w - T_{aw}) C_H \quad A-7$$

where

$$T_{aw} = T + \frac{u^2}{2C_p} \quad A-8$$

The heat transfer coefficient is related to the friction coefficient by Reynold's analogy.

$$C_H = \frac{1}{2} C_f \quad A-9$$

For circular vehicle and tube the relations for A_{ww} and A_{vw} are

$$\frac{1}{A} \frac{dA_{ww}}{dx} = \frac{4}{d(1 - \beta)} \quad A-10$$

$$\frac{1}{A} \frac{dA_{vw}}{dx} = \frac{4 \beta^{1/2}}{d(1 - \beta)} \quad A-11$$

The energy equation(A-3) can now be written in the form

$$\left(C_p \frac{dT}{dx} + v \frac{dv}{dx} \right) \rho v = \frac{2C_f}{d(1-\beta)} \left[\rho u |u| u_s - \frac{\rho}{2} u^2 |u| + \rho |u| C_p (T_w - T) \right] \quad A-12$$

By introducing

$$T_o = T + \frac{v^2}{2C_p} \quad A-13$$

and

$$T_{ow} = T_w + \frac{u_s^2}{2C_p} \quad A-14$$

the energy equation can be written in the form

$$\rho v \frac{dT_o}{dx} = \frac{2C_f \rho |u|}{d(1-\beta)} (T_{ow} - T_o) \quad A-15$$

A simple solution to this equation is $T_o = T_{ow}$ which is a constant. This solution is the correct one if the initial conditions in front of the vehicle are such that the stagnation temperature of the air is the value it would have if it were at wall temperature and moving at wall velocity.

Far from the vehicle where the fluid is undisturbed by the vehicle, the temperature of the fluid in the tube is equal to the temperature of the tube wall and the condition given by Equation A-15 is satisfied so that there is no net energy transfer with the tube wall. The condition is not that the heat transfer with the wall is zero, but that the heat transfer with the wall is enough to balance the energy transfer caused by the frictional shear force acting on the moving tube wall. The tube wall will be warmed by this heat transfer but, for values of gas densities equal to one atmosphere or less and reasonable estimates of tube wall heat capacities, there would not be an appreciable

change in wall temperature. If the steady flow solution holds from far ahead of the body to the vicinity of the body, then the stagnation temperature of the gas in the vehicle fixed coordinate system would be a constant. For the isentropic expansion of the flow into the annular passage about the vehicle, the stagnation temperature would remain constant, and for the flow through the annulus with friction and heat transfer the stagnation temperature would continue to be constant, if there is no energy exchange with the vehicle. Since the vehicle is stationary in this coordinate system, the drag force of the vehicle is not an energy input to the flow. For this condition, the entire flow within the tube follows the constant stagnation temperature Fanno line conditions. The assumption of constant stagnation temperature about the vehicle, which one might have assumed by neglecting energy transfer with the walls, is indeed justified if this energy transfer is considered.

The long time steady flow condition in front of the body need not hold for all conditions. Soon after the initiation of motion, the conditions in front of the vehicle would be expected to be isentropic and continue to be so until the waves generated by the vehicle have penetrated a long way down the tube and friction and heat transfer with the walls have become important. Unsteady isentropic waves that are moving with respect to the coordinate system will cause a change in stagnation temperature. Equation A-15 shows that if the stagnation temperature in the flow is different than its undisturbed value, then there will be a net energy transfer with the tube wall and the stagnation temperature through the annular passage will not be constant.

The steady flow of a fluid in a tube or annulus with one wall in motion and friction and heat transfer has several interesting features. While all of these features are not of direct practical importance to the tube vehicle problem, it is of interest to consider them briefly. With a moving wall, the friction force may act either in the direction of flow or against the direction of flow. Under these conditions there are two families of constant stagnation temperature flows. The usual one in which the friction force is against the direction of motion occurs in the annulus about the vehicle and causes the flow to accelerate. The solution which is of interest in the flow ahead of the vehicle is the one for which the friction force is

in the direction of the flow velocity and the fluid decelerates. Far ahead of the vehicle the fluid is at rest with respect to the tube. This at rest condition is unstable in the sense that a small perturbation will grow as one moves along the tube. If the flow velocity is slowed down slightly with respect to the tube, then the fluid velocity will continue to decrease in a downstream direction. If the fluid velocity is increased with respect to the tube, then the sign of the friction term will be reversed and the fluid will continue to accelerate in the downstream direction.

2. VEHICLE DRAG AND MOMENTUM LOSS

If the flow about the vehicle is adiabatic, then the stagnation enthalpy or temperature of the flow is a constant in vehicle fixed coordinates and the solution to the energy equation is quite simple. The only complications exist in the momentum equation. The fluid exerts a drag force on the vehicle which is balanced by a thrust which is applied to the vehicle. The fluid incurs a momentum loss in flowing about the vehicle which is caused by the drag exerted on the vehicle and on the tube wall. The friction force on the tube wall affects the vehicle drag by causing an increase in the pressure drop along the annular passage. This increased pressure drop causes a lower pressure on the base of the vehicle and consequently an increase in the drag of the vehicle. The direct friction force on the tube wall does not affect the vehicle drag except as it acts through the pressure effect. The momentum loss of the fluid in flowing around the vehicle is affected by both the force that the vehicle exerts on the fluid, its drag, and the force that the wall exerts on the fluid. The momentum loss of the fluid and the drag on the vehicle differ by the amount of the friction force on the tube wall. This tube wall friction force is different than would occur in the same length of tube without the presence of the vehicle, since the fluid velocities in the annular passage about the vehicle are different than in the tube without the vehicle. For the calculation of fluid dynamic properties in the tube, the total momentum loss which occurs as the fluid flows around the vehicle is important. The drag on the vehicle is also important since it must be balanced by a thrust.

3. NOSE AND TAIL LOSSES

Any loss in stagnation pressure taking place either about the nose or

the tail of the body would increase the momentum loss and vehicle drag. In this study no nose loss has been assumed and the tail loss has been calculated by assuming the base pressure to be equal to the pressure in the annular passage at the base of the vehicle which is appropriate for a blunt base vehicle.

The possibility of a loss at the nose of the body has been considered in several of the experimental studies of near flowfield tube vehicle aerodynamics. In the studies performed by Gouse et al at MIT and Carnegie-Mellon Institute (Reference 9), the presence of a loss in stagnation pressure at the nose was not measured or considered. In the later work at GASL, (Reference 6), a nose loss coefficient was interpreted from the measured pressure distributions. This same approach was used in the experiments run at JPL (Reference 7). In the JPL results, the nose loss was sometimes found to be a gain. Under this condition it was not considered to represent a change in stagnation pressure but a departure from the one dimensional flow assumption that was used in reducing the data. However, experience with orifices has shown that with a small amount of rounding of the inlet, separation can be avoided and an essentially loss free entrance accomplished. The available experimental data for tube vehicles does not appear to justify a change in this result especially since there does not seem to be any plausible reason for such a change.

A base pressure equal to the pressure in the annulus at the base of the vehicle seems to have been the assumption used in reducing all of the experimental studies referenced. The experimental studies, however, do not appear to be good enough to confirm the validity of this assumption. This assumption is the one which is classically used in low speed incompressible flow and is used in deriving the Borda-Carnot loss for a sudden expansion. This same condition appears to be valid for all subsonic annulus exit speeds. When sonic velocity is reached at the exit of the annulus, the flow can expand supersonically into the base region resulting in a reduced base pressure. This is the mechanism that can lead to the increase in drag coefficient that takes place for the choked flow condition. As has been discussed elsewhere, the base flow is then determined by the conditions set by the far flowfield and cannot be determined by near flowfield considerations.

SOLUTION OF THE NEAR FLOWFIELD

The solution of the near flowfield is accomplished by first calculating the conditions at the entrance to the annulus by an isentropic expansion from the cross sectional area of the tube to the area of the annulus. The flow equations with friction and heat transfer are then integrated through the annulus to the base. If the Mach number at the base has not yet reached one, the momentum loss coefficient and drag coefficient can then be calculated. These coefficients are calculated by taking the difference of the momentum flux at the base of the body from that at the nose of the vehicle for the momentum loss and subtracting the friction on the tube wall from the momentum loss to obtain the drag. Increased relative Mach number, increased blockage ratio, or increased friction along the annulus will cause an increase in exit Mach number. The choking Mach number is obtained by finding the value of relative Mach number for which Mach number one occurs at the exit. Calculations should not be made for higher values of relative Mach number since Mach number equal to one will be reached before the base of the vehicle and the integration of the equations cannot be continued beyond this point.

If the flow quantities are nondimensionalized by the ambient conditions in the tube, equations A-1 through A-15 can be combined to give

$$\frac{v^*}{p^*} \frac{dp^*}{dv^*} = \frac{\left(\frac{|u|u^*| + v|v^*|\beta^{1/2}}{v^{*2}} \right) \left[1 + (\gamma - 1) \frac{v^{*2}}{T^*} M_\infty^2 \right] + \frac{|u^*|}{v^*} \frac{T_w^* - T_{aw}^*}{T^*}}{\frac{|u^*|}{v^*} \left(\frac{T_w^* - T_{aw}^*}{T^*} \right) \frac{T^*}{v^*} \frac{1}{\gamma M_\infty^2} + \frac{|u|u^*| + v|v^*|\beta^{1/2}}{v^{*2}}} \quad \text{A-16}$$

$$\frac{1}{v^*} \frac{dv^*}{d\lambda} = \frac{\frac{|u^*|}{v} \left(\frac{T_w^* - T_{aw}^*}{T^*} \right) \frac{T^*}{v^{*2}} \frac{1}{M_\infty^2} + \gamma \frac{|u^*|u^*| + v^*|v^*|\beta^{1/2}}{v^{*2}}}{\frac{T^*}{v^{*2}} \frac{1}{M_\infty^2} - 1} \quad \text{A-17}$$

where

$$v^* = \frac{v}{u_s}, \quad u^* = \frac{u}{u_s}, \quad M_\infty = \frac{u_s}{\sqrt{\gamma R T_w}}, \quad p^* = \frac{p}{p_\infty}$$

The conditions at the entrance to the annulus can now be found for any particular set of conditions just ahead of the vehicle by the isentropic flow relations between these two points. These conditions are then used as the initial conditions from which to integrate equations A-16 and A-17. The momentum loss coefficient can then be calculated by the relation

$$C_{MT} = \frac{1 + \gamma M_1^2 - \frac{p_e}{p_1} [(1 + \gamma M_e^2)(1 - \beta) + \beta]}{\frac{\gamma}{2} M_1^2}$$

The frictional effects are all contained in the parameter

$$\lambda = \frac{2C_f L}{(1 - d)}$$

so that a family of vehicles of different length and friction coefficient all have the same value of λ and the properties of all these vehicles can be obtained from this one calculation.

APPENDIX B

FAR FLOWFIELD SOLUTION

1. FLOWFIELD EQUATIONS

The equations that describe the far flowfield are those of one dimensional unsteady compressible flow. The equations can be written as follows:

$$\text{Continuity} \quad \frac{\partial \rho}{\partial t} + \rho \frac{\partial u}{\partial x} + u \frac{\partial \rho}{\partial x} = 0 \quad \text{B-1}$$

$$\text{Momentum} \quad \frac{\partial u}{\partial t} + u \frac{\partial u}{\partial x} + \frac{1}{\rho} \frac{\partial p}{\partial x} + F = 0 \quad \text{B-2}$$

$$\text{Energy} \quad \frac{\partial \rho}{\partial t} + u \frac{\partial p}{\partial x} - C^2 \left(\frac{\partial \rho}{\partial t} + u \frac{\partial \rho}{\partial x} \right) = (\gamma - 1) \rho (q + uF) \quad \text{B-3}$$

$$\text{State} \quad p = \rho RT \quad \text{B-4}$$

$$\text{Friction} \quad F = \frac{2C_f}{d} u|u| \quad \text{B-5}$$

$$\text{Heat Transfer} \quad q = \frac{4C_H}{d} C_p |u| (T_w - T_{aw}) \quad \text{B-6}$$

These equations have the property that, along special directions in the x, t plane called characteristic direction, they can be written in the form of total differential equations and integrations of these total differential equations carried out along these directions. There are three characteristic directions.

The first two directions are given by: $\frac{dx}{dt} = u \pm C$ B-7

And the third direction by: $\frac{dx}{dt} = u$ B-8

The first two directions are those taken by disturbances that travel with the speed of sound to either left or right. The third characteristic direction is that of a particle path. Pressure waves follow the characteristics which move with the speed of sound while entropy effects follow the particle paths. The equations that determine the changes in fluid properties along these characteristic directions are as follows:

$$du = \bar{+} \frac{2}{\gamma - 1} dc + \left[\pm \gamma \frac{q}{c} - F \left(1 \mp \frac{u}{c} \right) + \frac{C^2}{\gamma} \frac{\partial}{\partial x} \left(\frac{s}{R} \right) \right] dt$$
 B-9

along the first two characteristics and

$$(ds)_{\text{path}} = \frac{uF + q}{T} (dt)_{\text{path}}$$
 B-10

along the third characteristic.

These equations can be solved by calculating the direction of the characteristics and the changes that take place along the characteristics. Since the direction of the characteristics depend upon the fluid flow conditions and the changes along the characteristics depend upon the locations of the characteristic mesh points, these solutions are mutually dependent and must be carried out in an iterative fashion.

In the present analysis the assumption is made that the local heat transfer and skin friction depend only on the mean flow properties in the tube and that they are independent of the time rate of change of these properties.

This assumption appears to be justified for the rate of change of properties experienced in this problem. However, there is really not yet enough data on the effects of unsteady flow on heat transfer and friction to properly assess this assumption. The friction coefficient is determined by first calculating the Reynolds number and then determining the skin friction coefficient by the relation

$$C_f = \frac{16}{Re_d} \quad Re_d < 2500 \quad B-11$$

for a laminar flow condition and

$$4 \log_{10} [2Re_d C_f^{1/2}] - 1.6 = C_f^{-1/2} \quad Re_d > 2500 \quad B-12$$

for a turbulent flow condition. The friction coefficient as a function of Re_d is shown in Figure B-1. The heat transfer coefficient is then determined by Reynold's analogy which gives

$$C_H = \frac{C_f}{2} \quad B-13$$

While the amount of friction and heat transfer, which takes place when flow is laminar is small, the laminar flow relations are important to a proper solution of the problem. Since the actual heat transfer rate is given by equation B-6, the heat transfer will go to zero as the velocity goes to zero unless the laminar flow heat transfer relation is used which gives an infinite heat transfer coefficient at zero flow velocity. This condition insures that the fluid will eventually return to the temperature of the tube wall which it obviously must in the real problem.

2. SOLUTION FOR CONDITIONS ABOUT THE VEHICLE

An appropriate set of boundary conditions must be placed on the far flowfield which are compatible with the near flowfield solution for flow about the vehicle. For purposes of the far flowfield solution the

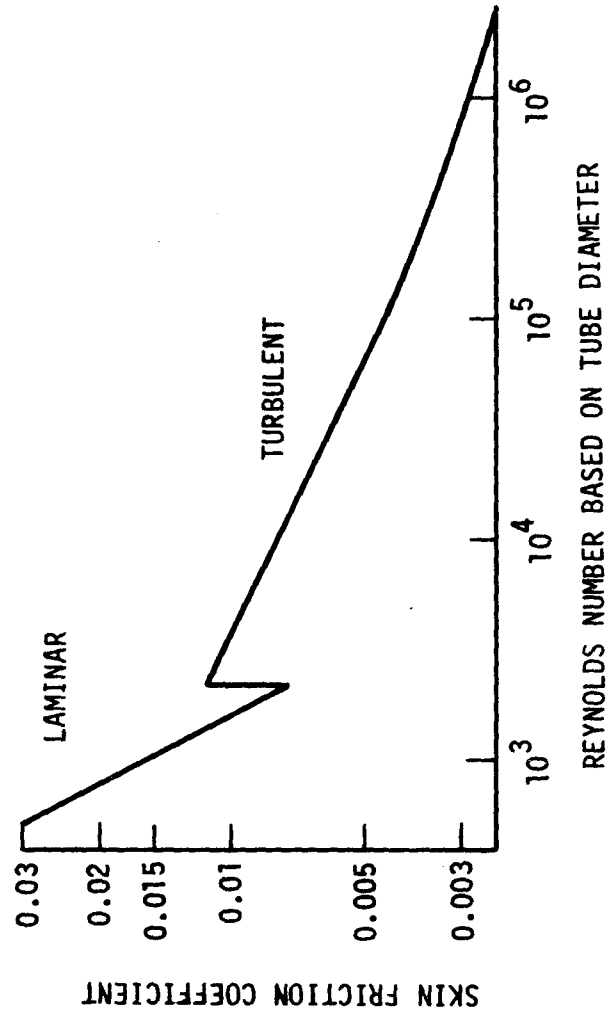


Figure B-1. Friction Coefficient as a Function of Reynolds Number

only input needed from the near flowfield solution is the momentum loss as a function of the relative Mach number (and other appropriate flowfield conditions) and the choking Mach number. An analytical relation is fitted to the momentum loss coefficient Mach number curve to describe this information to the far flowfield solution. The solution to the fluid properties about the vehicle must then be obtained in two ways depending on whether the relative Mach number is at or below the critical value. First consider the case for which the relative Mach number is below the choking value. Since the flow is considered to be steady about the body, the equations for the fluid properties are as follows:

$$\text{Continuity} \quad \frac{P_2}{a_2^2} (u_2 - u_s) = \frac{P_1}{a_1^2} (u_1 - u_s) \quad \text{B-14}$$

$$\text{Energy} \quad \frac{a_2^2}{\gamma - 1} + \frac{(u_2 - u_s)^2}{2} = \frac{a_1^2}{\gamma - 1} + \frac{(u_1 - u_s)^2}{2} \quad \text{B-15}$$

$$\text{Momentum} \quad P_1 - P_2 + \frac{\gamma P_1}{a_1^2} (u_1 - u_s)^2 - \frac{\gamma P_2}{a_2^2} (u_2 - u_s)^2 = \frac{D}{A} \quad \text{B-16}$$

The point at the front of the vehicle must also lie on a left running far flowfield characteristic and that at the back of the vehicle on a right running characteristic (Figure B-2). The relations along these characteristics are given by equations B-9. This set of equations together with the relation between drag and Mach number obtained from the near flowfield solution forms a complete set for determining the properties about the vehicle. The equations do not allow an explicit solution. An iterative method has been adopted for their solution. A value of the relative Mach number in front of the vehicle is assumed based on the relative Mach number at the last point calculated. The conditions in front of the body are then determined using equation B-9 along the left running characteristic from a

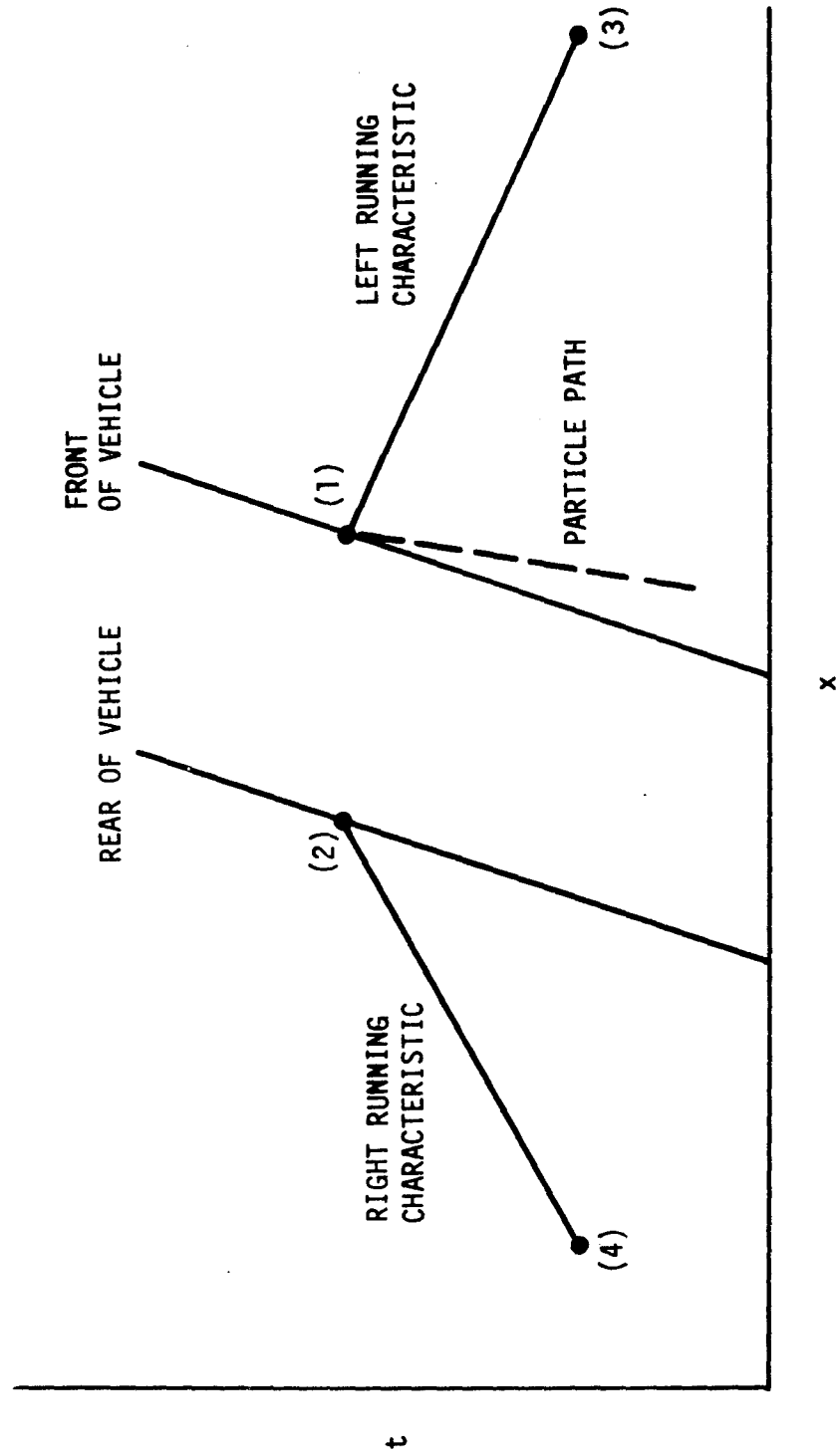


Figure B-2. Time-Distance Diagram of the Vehicle Boundary Condition for the Far Flow Field

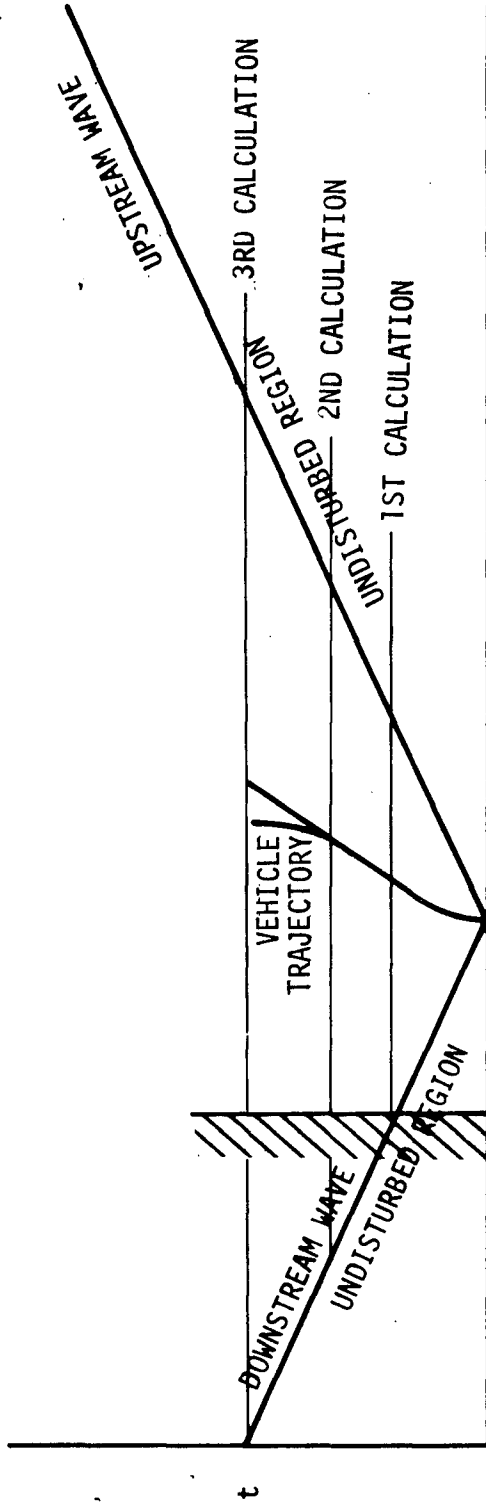
known point (3) and equation B-10 along the particle path. Knowing the conditions in front of the vehicle, the conditions behind the vehicle can then be determined using equation B-14 through B-16. The momentum loss coefficient is determined from the relation derived from the near flowfield if the Mach number is less than the critical value. The conditions behind the vehicle are then checked for compatibility with the previously determined conditions behind the body point (4) using relation B-9 along a right running characteristic. If this condition is not compatible, a new value of Mach number is selected and iteration continued until agreement is reached. This process is valid as long as the relative Mach number in front of the vehicle is less than the choking value. In the iterative process of determining the relative Mach number in front of the vehicle, the Mach number should never be set equal to a value larger than the choking Mach number. When the relative Mach number is equal to the choking value, any value of the momentum loss coefficient greater than the minimum value at the choking Mach number is acceptable. The Mach number is kept at the choking value and a value of the momentum loss coefficient larger than the minimum value at the choking Mach number is selected. Conditions behind the vehicle are then calculated as before and checked for compatibility. The value of the momentum loss coefficient is iterated until a compatible result is obtained.

3. METHOD OF SOLUTION

The method by which the solution is accomplished is designed to provide the flexibility required to handle a wide range of tube train problems. The method is designed to allow a close mesh spacing of points in the regions where there are rapid changes in flow conditions and a broader spacing in the regions in which conditions are changing only slowly and such close spacing is not required. The advantage of this variable spacing is that it allows a more accurate answer to be obtained with a given expenditure of funds for computing. The method also allows a run to be terminated after a specified duration of vehicle travel and the results examined. The run can then be continued if so desired. This capability allows the runs to be made in short sections so that the results can be examined during the run and large amounts of computing time are not wasted on abortive runs. It also allows different conditions to be used to

complete the same initial run with the result that the effects of different end conditions can be determined based on the same initial results without recomputing. For example, a vehicle can be started and accelerated up to cruising speed and travel a specified distance down the tube in one run. During this period the disturbance generated by the vehicle will reach a limited distance down the tube. This run can then be continued in several different ways. A tube end may be located at any position beyond the limit of the initial region of influence, and the vehicle may be continued at cruise velocity for any specified distance before being decelerated. Figure B-3 further illustrates this means of making calculations.

The starting point for all tube vehicle calculations is the vehicle at rest in the tube. For the initial run of the vehicle, the fluid throughout the tube should be at rest and at uniform ambient conditions. The vehicle is then started and follows some velocity trajectory. In this calculation, it was chosen to specify the velocity instead of the propulsive force or power since this method gives a simpler calculation and it appeared easier to specify rational velocity trajectories beforehand. Other means of specifying the vehicle trajectory could be used if and when these became desirable. The region in which the fluid in the tube can be influenced by the motion of the vehicle lies between the up and downstream characteristics which originate from the vehicle at the start of the vehicle motion (Figure B-3). For ambient tube conditions, conditions along these characteristics are specified as ambient and the spacing of points along these characteristics is specified. A maximum time of vehicle travel is specified. The computer program now calculates the fluid and vehicle conditions between the two initial characteristics up to the maximum time specified. This result can be printed in digital form, plotted, and also is recorded on tape. During the initial acceleration phase of the vehicle travel, relatively strong disturbances are developed which are transmitted out along the characteristics. A relatively close mesh spacing is needed in this region to accurately predict the fluid disturbances. If a constant cruise speed follows this region of acceleration, the new disturbances caused are much weaker and a coarser mesh may be used without loss in accuracy. A computer run can be made up to some maximum time using an appropriately selected mesh spacing. This run is then terminated and the results examined. This run can then be continued in any of several ways.



- 1) VEHICLE ACCELERATES TO CRUISING SPEED IN 1ST CALCULATION
- 2) A TUBE END MAY BE PLACED AT OR OUTSIDE THE DOWNSTREAM LIMIT OF WAVE PROPAGATION AND 2ND CALCULATION MADE BOTH WITH OR WITHOUT TUBE END
- 3) THE VEHICLE MAY DECELERATE AFTER THE END OF THE 2ND CALCULATION OR IT MAY CONTINUE AT CONSTANT VELOCITY. EITHER OF THE 2ND CALCULATIONS MAY BE CONTINUED WITH EITHER VELOCITY PROFILE

Figure B-3. Time-distance diagram illustrating the way in which different boundary conditions can be used to satisfy a variety of conditions from the same initial calculation.

Tube ends can be located at any point outside of the region which has been influenced. For instance, tube ends can be located at the boundaries of the region of influence. The calculation can then be restarted and continued without supplying any additional information on fluid conditions in the tube. The vehicle velocity history should be specified up to the maximum time for which the calculation is desired. Another possible way to continue the calculation would be not to specify any tube ends but continue the data out along the initial characteristics to some new maximum time. The calculation would then be for the case in which the ends of the tube are beyond the region influenced at the new maximum time. In the next step the calculation can be carried on even further, again with the option of locating ends within the new expanded region of influence or not as desirable. Another possible option is to continue a run using different vehicle velocity histories. In this way it is possible to examine the changes caused by tube ends and different velocity histories without making entirely new runs.

APPENDIX C

EFFECT OF HEAT TRANSFER

The importance of including the heat transfer term is probably intuitively less obvious than the effect of the friction term. The friction term enters in both the momentum and the energy equations while the heat transfer term enters only in the energy equation. Judging from the fact that the entropy is negative in front of the vehicle, the heat transfer effect would appear to be the more important one. For a choked vehicle it can be shown that the pressure in front of the body for the asymptotic long time solution depends on the entropy. Using the relation for entropy

$$s - s_{\infty} = C_V \ln \frac{T}{T_{\infty}} - R \ln \frac{\rho}{\rho_{\infty}} \quad \text{C-1}$$

The continuity equation

$$\rho_{\infty} V_{\infty} = \rho V \quad \text{C-2}$$

and the equation of state, the pressure in front of the vehicle for which the flow is choked can be expressed directly in terms of the entropy and the ratio of the vehicle to choking Mach numbers. The result is

$$\frac{p}{p_{\infty}} = \left(\frac{M_{\infty}}{M_c} \right)^{2\gamma/(\gamma+1)} \exp \left[- \frac{\gamma-1}{\gamma+1} \frac{s - s_{\infty}}{R} \right] \quad \text{C-3}$$

If heat transfer with the wall did not take place, the entropy in front of the body has to be larger than the initial value in the tube. There appears to be no simple way for estimating how much larger, but the initial value is certainly a minimum. Therefore, a minimum value of the long time asymptotic pressure for the Case 4 without heat transfer would be

$$p_1/p_{\infty} = 2.92$$

while the value with heat transfer is

$$\frac{p}{p_{\infty}} = 2.55$$

This increase in pressure by 15% or more should cause a corresponding increase in drag.

The heat transfer is also important for predicting the long time conditions behind the vehicle. Heat transfer is essential if the final temperature and pressure in the tube are to return to the initial values.

The relative magnitude of the heat transfer and friction effects in the energy equation can be easily compared. The energy supplied to the flow by the friction effect is τu_s and that by heat transfer is q . The ratio of these two effects can be compared using Reynold's analogy.

$$\frac{q}{\tau u_s} = \frac{C_p (T_{aw} - T)}{u u_s}$$

For a vehicle velocity of 293 ft./second, and an induced velocity of 100 ft./second, the effect of heat transfer exceeds the friction for a temperature difference of

$$T_{aw} - T = 4.9^{\circ}\text{R.}$$

REFERENCES

1. A. G. Hammitt, "The Aerodynamics of Vehicles Passing Through Tunnels," Proceeding of the International Symposium on the Aerodynamics and Ventilation of Vehicle Tunnels, BHRA Fluid Engineering, Cranfield, Bedford, England, 1973.
2. J. A. Fox and A. E. Vardy, "The Generation and Alleviation of Air Pressure Transients Caused by the High Speed Passage of Vehicles Through Tunnels," BHRA Fluid Engineering, Cranfield, Bedford, England, 1973.
3. C. R. Strom, "An Analytical Procedure for Calculating the Aerodynamic Performance of Vehicles Traveling in Tunnels," The MITRE Corporation, McLean, Virginia, Prepared for DOT, PB 220 082, December 1972.
4. A. G. Hammitt, "Aerodynamic Analysis of Tube Vehicle Systems," AIAA Journal, Vol. 10, No. 3, pp. 282-290, March 1972. (similar to PB 178 796)
5. A. G. Hammitt, "The Aerodynamics of High Speed Ground Transportation," Western Periodicals Company, 13000 Raymer Street, North Hollywood, California, 1973.
6. D. E. Magnus and S. Panunzio, "Analysis of the Near Flowfield for High Speed Vehicles in Tubes," AIAA Paper 70-140, New York, 1970. (similar to PB 198 205)
7. B. Dayman and D. W. Kurtz, "Experimental Studies Relating to the Aerodynamics of Trains Traveling in Tunnels at Low Speeds," Proceeding of the International Symposium on the Aerodynamics and Ventilation of Vehicle Tunnels, BHRA Fluid Engineering, Cranfield, Bedford, England, 1973. (similar to UMTA-DC-06-0010-72-13 and UMTA-DC-06-0010-72-14)
8. F. T. Brown, et al., "Unsteady Flow in Tubes and Tunnels," Department of Mechanical Engineering, Massachusetts Institute of Technology, Cambridge, Massachusetts, Prepared for DOT, PB 204 584, August 1971. (similar to PB 204 584)
9. R. G. Hoppe and S. W. Gouse, Jr., "Fluid Dynamic Drag on Vehicles Traveling Through Tubes," Prepared for DOT, PB 188 451.
10. C. R. Strom, "Letter, June 11, 1973, and Telephone Conversations," The MITRE Corporation, McLean, Virginia
11. Edward J. Ward, "Letter, August 27, 1973, Federal Railroad Administration," Department of Transportation, Washington, D. C.

